

Determining the Constants for and Analyzing the Predictive Capabilities
of a Gas Sorption Model for Semi-Crystalline Polymers

by

JEFFREY DAVID PFEIFLE

Submitted to the Department of Mechanical Engineering
in Partial Fulfillment of the Requirements for the Degree of

Bachelor of Science
in Mechanical Engineering

at the

Massachusetts Institute of Technology

February 1992

© Jeffrey David Pfeifle, 1992. All rights reserved.

The author hereby grants to MIT permission to reproduce and to
distribute copies of this thesis document in whole or in part.

Signature of Author _____

Department of Mechanical Engineering
January, 1992

Certified by _____

Raiph E. and Eloise F. Cross Professor of Mechanical Engineering
Thesis Supervisor
Nam P. Suh

Accepted by _____

Peter Griffith
Chairman, Department Thesis Committee

ARCHIVES
MASSACHUSETTS INSTITUTE
OF TECHNOLOGY

MAY 05 1992

LIBRARY

Determining the Constants for and Analyzing the Predictive Capabilities
of a Gas Sorption Model for Semi-Crystalline Polymers

by

JEFFREY DAVID PFEIFLE

Submitted to the Department of Mechanical Engineering
in Partial Fulfillment of the Requirements for the Degree of
Bachelor of Science
in Mechanical Engineering
at the
Massachusetts Institute of Technology

February 1992

ABSTRACT

The increasing level of technology in the materials industry has led to the development of many new materials. Microcellular foamed plastic is a semi-crystalline polymer developed in the last decade. An understanding of this material and of the gas sorption method by which it is formed are vital to fully utilizing its capabilities.

A gas sorption model which attempts to predict the spatial distribution of gas and the crystalline morphology of a sample over time is studied and the theory behind the model is explored. The constants of the crystallinity model were solved for gas sorption of PET at 800 psig and 25° C. Eighteen PET samples were exposed to gas saturation at the same pressure and temperature, but various saturation times between 5 and 400 hours. The samples were analyzed by a Differential Scanning Calorimeter (DSC) to determine the sample crystallinity. The scanning rate was 20° C/minute.

The results of the gas sorption model prediction and the experimental results were compared to determine the model accuracy. Experimental results showed a maximum crystallinity of 30% and a main crystallization period occurring between 10 and 30 hours. The gas sorption model predicted a maximum of 25% crystallinity and a main crystallization period occurring between 20 and 100 seconds.

The comparison of the model to the experimental results indicated the need to explore further the gas sorption of semi-crystalline polymers at room temperatures. Due to the lack of data available, the crystallinity model's time constant could not be found.

Thesis Supervisor: Nam P. Suh

Title: Ralph E. and Eloise F. Cross Professor of Mechanical Engineering

I dedicate this thesis to my sister, whose constant faith and love has provided me with strength through all these years.

Christie, may you have the opportunities to achieve your goals, and may you always know that I will be here for you.

Acknowledgements

I thank my family for always being there when I needed them and for providing me with the resources necessary to achieve my goals.

I thank my friends, who cheerfully goaded me on, and wished me well in my endeavor to graduate.

I thank Dan Baldwin for sparking my interest in this project and for taking the time to lend a hand when I needed one. I thank Chul Park for making me feel welcome about the lab.

I thank the member companies of the MIT-Industry Microcellular Plastics Consortium for their support.

And I thank Peggy Garlick, without whose help this thesis surely would never have come about.

Table of Contents

Chapter 1 Introduction

1.1 Microcellular Foamed Plastics	8
1.2 Gas Sorption	9
1.3 Polyethylene Terephthalate	10
1.4 Crystallization	13
1.5 Intent	16

Chapter 2 Theoretical Models

2.1 Modeling Gas Sorption in Semi-Crystalline Polymers	17
2.2 Diffusion Model	18
2.3 Crystallization Model	19
2.4 Crystallinity Calculation	20

Chapter 3 Solving the Crystallization Model

3.1 Calculating the Potential Energy Change	22
3.1.1 The Potential Energy Change at 120° C	22
3.1.2 The Potential Energy Change at 25° C	24
3.2 Finding the Spherulite Growth Rate	26
3.2.1 Experimental Analysis	26
3.2.2 Theoretical Analysis	29
3.3 Finding the Spherulite Nucleation Rate	31
3.3.1 Calculating the Initial Spherulite Nucleation Density Rate	32
3.3.2 Modeling the Reciprocal Nucleation Time Constant	33
3.3.3 Applying the Spherulite Nucleation Rate	34
3.3.4 Finding the Spherulite Nucleation Activation Energy	39
3.3.5 Solving for the Spherulite Nucleation Rate	39
3.4 Analytically Predicting the Mass Fraction of Crystalline Material	40

Chapter 4 Experimental Method and Results

4.1 Procedure	41
4.2 Apparatus	41
4.3 Results	42

Chapter 5 Verifying Model Prediction

5.1 Comparison of Model and Experimental Results	45
5.2 Discussion	46
5.3 Conclusions	47

Appendix A Nomenclature	48
-------------------------------	----

Appendix B Important Numbers	49
------------------------------------	----

Appendix C MathCad Calculation Sheets	50
---	----

Appendix D DSC Graphs	51
-----------------------------	----

References	70
------------------	----

Figures

Figure 1 Molecular Schematics of Polymers	10
Figure 2 Chemical Structure of PET	12
Figure 3 Chain-Folded Crystals	13
Figure 4 Progression of Spherulite Growth	14
Figure 5 Isotactic Polypropylene Sample Showing Crystalline Spherulites	15
Figure 6 Determining Spherulite Growth Rate and the Activation Energy Term by Experimentation	27
Figure 7 Model of Lamellar Growth Front Assuming Regular Chain-Folding	29
Figure 8 Determining Spherulite Growth Rate and the Activation Energy Term by Theory	30
Figure 9 Avrami Plot of Crystallization of PET at Various Temperatures	35
Figures 10 a,b,c,d Determining the Spherulite Nucleation Rate from Crystallinity and Density Terms	36-38
Figure 11 Gas Sorption Model Crystallinity vs. Time Plot	40
Figure 12 DSC Thermogram for PET Sample Saturated for 30 Hours at 800 psig and 25° C.	42
Figure 14 Crystallinity vs. Saturation Time for Kodak PET 9921	42
Figure 1 Gas Sorption Model Predicted Crystallinity Plot and that Found Experimentally	45

Tables

Table 1 Spherulite Growth Rate, \dot{r}_s , at Various Temperatures	27
Table 2 Avrami Constants of PET at Various Temperatures	35
Table 3 Spherulite Nucleation Rate, \dot{N} , for Various Temperatures	38
Table 4 Crystallinity and Weight Gain Calculations for PET Samples	43

Chapter 1 - Introduction

1.1 Microcellular Foamed Plastics

With the increased attention to issues of recyclability and materials cost, the modern manufacturing industry has been increasingly interested in finding ways to reduce the amount of material used in products while maintaining the original material properties. One solution which has been studied in the past decade is to incorporate microcellular foamed plastics into the manufacturing industry. Microcellular foamed plastics are foamed polymers characterized by voids less than 10 micrometers in diameter, as opposed to macrocellular foamed plastics, which have voids on the order of millimeters in diameter. Microcellular foamed plastics can have void fractions of up to 80%.

The benefits of working with microcellular foam are numerous. Because the voids are as much as two orders of magnitude smaller than those of macrocellular foamed plastics, parts made of microcellular foam can be much thinner and also have a smoother surface. The small void size allows for a substantial reduction in material, increasing the strength-to-weight ratio while preserving material properties. In fact, because the void size is less than that of pre-existing defects in the material, many of the material properties improve. Crack propagation resistance is increased because of the small void size; cracks that encounter a void do not continue to propagate because a small void easily deforms and stores the elastic energy of the crack tip instead of allowing it to continue. This process of crack tip blunting is also responsible for increases in impact strength and fracture toughness [14].

Much of the research in past years has dealt with making the manufacturing processes of microcellular foam commercially available. The processes generally studied have been thermoforming, extrusion and injection molding. However, some research has focused on understanding the process of creating microcellular foam. This thesis is based on such research, and in particular on the mechanics of CO₂ gas sorption.

1.2 Gas Sorption

In the last seven or eight years, the process of inducing crystallization through CO₂ gas sorption in order to produce microcellular foamed plastics has been studied by many researchers [4, 7].

Gas sorption is the process of exposing a polymer to gas under pressure, usually at an elevated temperature. The differential of the gas concentration outside the polymer and within causes the gas to diffuse into the polymer. Because of the elevated temperature, the gas is free to move within the polymer and gas molecules slowly come together and form nuclei within the material. When the polymer is removed from the pressurized gas environment and allowed to cool, it begins to crystallize at the nucleation sites and forces the gas out of the polymer matrix and into small cells, or voids, which grow to slightly less than 10 micrometers in diameter.

The study of gas sorption has provided a new approach to creating crystallinity in polymers. One important aspect of this new approach deals with the amount of control over crystallization that can be exerted. While the diffusion rates and the extent of sorption in polymers for both liquids and vapors are governed by their saturation states, the amount of gas sorption into a polymer can be increased by elevating the pressure of the gas. This effect allows the rate and extent of crystallization caused by exposure to a gas to be controlled by adjusting the pressure, providing much more flexibility and control in materials processing of polymers, and making the creation of materials like microcellular foamed plastics possible.

While polymethyl methacrylate (PMMA) and polyvinylidene fluoride (PVF₂) were the materials first studied with gas sorption, polyethylene terephthalate (PET) is often used today, and is the polymer examined in this thesis.

1.3 Polyethylene Terephthalate

A polymer, whether thermoplastic, thermoset, or elastomer, is made up of long chain-like molecules in which the atoms forming the chain backbone are linked by covalent bonds. Usually, these covalent backbones are composed of carbon atoms. Weak Van der Waals and hydrogen bonds link the remainder of the polymer molecules. Some polymers also contain cross-links, formed by the stronger covalent bonds.

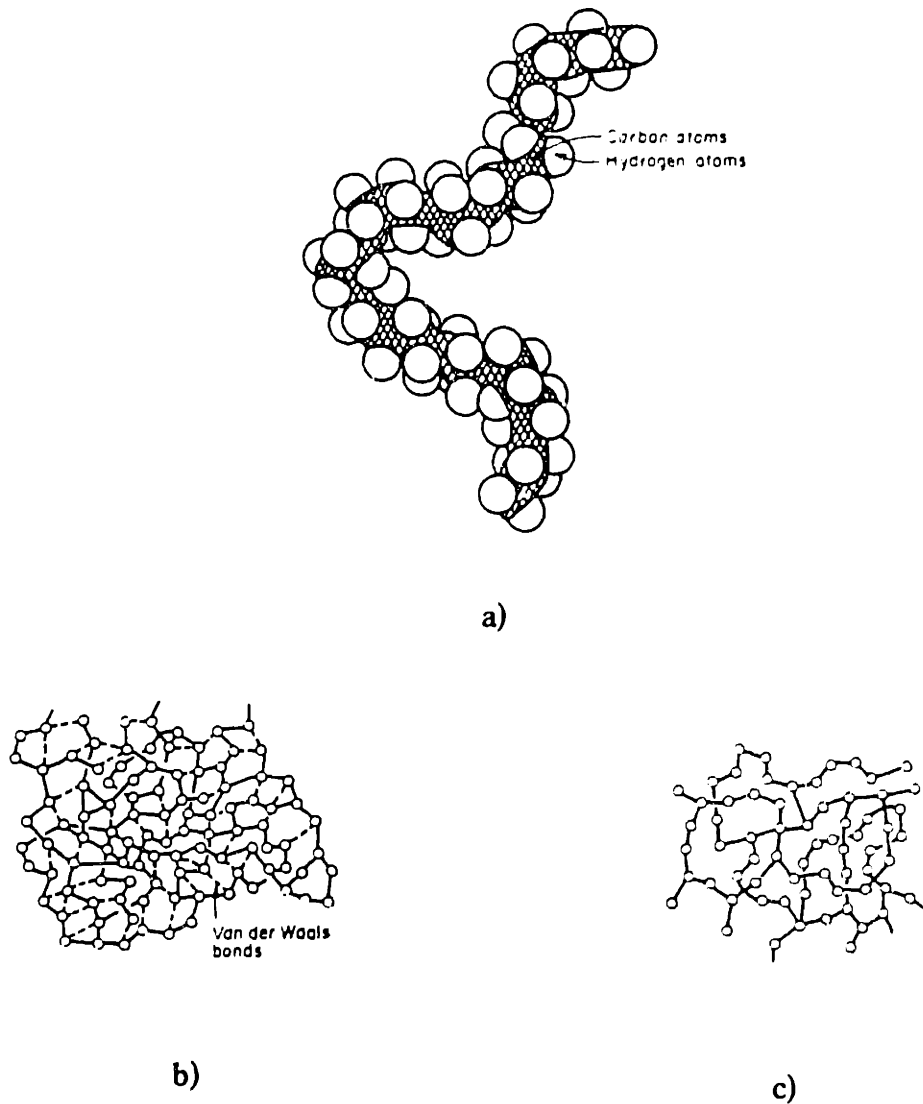


Figure 1 a) short bit of polyethylene molecule b) rubber linked with many secondary bonds c) polymer (like epoxy resin) where the chains are tied by frequent cross-links [1]

Thermoplastics are often described as linear polymers because of their lack of cross-links. Because of this lack, thermoplastics soften upon heating; the secondary bonds which bind the molecules to each other weaken so that the plastic flows like a viscous liquid. Thermosets are heavily cross-linked polymers sometimes described as network polymers. The strong cross-links prevent true melting or viscous flow so the polymer cannot be hotworked; it will turn into a rubber and, upon further heating decompose. Elastomers are near-linear polymers with occasional cross-links. At room temperature, elastomer secondary bonds have already melted and the polymer flows when loaded. The cross-links provide the material memory so that it returns to its original shape on unloading. Thermoplastics, particularly PMMA, PVF₂ and PET, are usually used in gas sorption experiments.

Thermoplastics are made by polymerizing monomers, or chain sub-units, together to form long chains. All of these chains have a carbon backbone, many contain hydrogen, and some contain fluorine, oxygen, chlorine and nitrogen. Polyethylene, polypropylene, polystyrene and nylon are all thermoplastics.

In many thermoplastics, the monomer chains are arranged randomly and not in regular repeating three-dimensional patterns. Such thermoplastics are amorphous. In other thermoplastics, the chains can be folded backwards and forwards over one another. The regularly repeating symmetry of this chain folding leads to long-range order and is termed crystallinity. Some thermoplastics contain both amorphous and crystalline regions, and are called semi-crystalline. Polymers do not crystallize 100% like inorganic materials.

Polyethylene terephthalate (PET) is termed a fibre and film-forming thermoplastic, one of a more complex structure than that of the other thermoplastics. It exists in an amorphous state, an oriented, partially crystalline state, and a highly crystalline state. It is a very useful, tough, and versatile thermoplastic which is widely used. The chemical structure of PET depends upon its starting material and is shown in Figure 2.

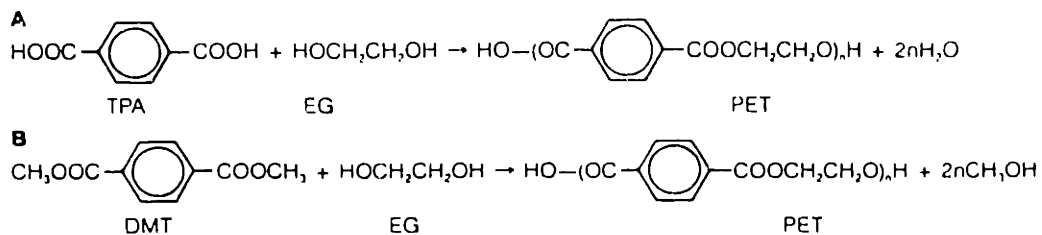


Figure 2 Chemical structure of PET, using terephthalic acid (A) or dimethyl terephthalate (B) and ethylene glycol as starting materials. [6]

PET is used in two-liter bottles, its shatterproof nature and creep-resistance making it an ideal material. A PET bottle also weighs about 1/13 as much as a glass bottle of the same size. Another common use for PET is the making of crystalline trays for both microwave and conventional oven use. PET can also be found in X-ray and photographic film, electrical insulation and food film packaging.

Typically, PET is formed through high-temperature extrusion, molding, fiber spinning, or film processing. The development of the technology to blow mold amorphous preforms was integral to the beverage bottle market. PET has also fit well into the thermal forming process, requiring only the use of hot molds to produce crystalline products. Perhaps the only true difficulty in using PET is the necessity to dry it during processing to prevent hydrolysis and the loss of material integrity.

Pioneer work on the study of PET as a gas sorption material was done by J.S. Chiou and others in 1985 [4]. Chiou chose PET as a test material because of its commercial importance and the previous literature on its vapor- and solvent-induced crystallization. His results were very similar to those reported by Lin and Koenig [9] for benzene-induced crystallization of PET. This study confirmed that a gas could be as effective as a solvent for inducing crystallization in certain polymers.

1.4 Crystallization

Polymer crystallization results from the folding of linear-chain molecules back upon themselves. Typically, as a polymer cools after being heated, secondary bonds tend to pull the molecules together into roughly parallel bundles. Under some circumstances, well defined chain-folded crystals form into thin pyramidal or platelike crystals called lamellae.

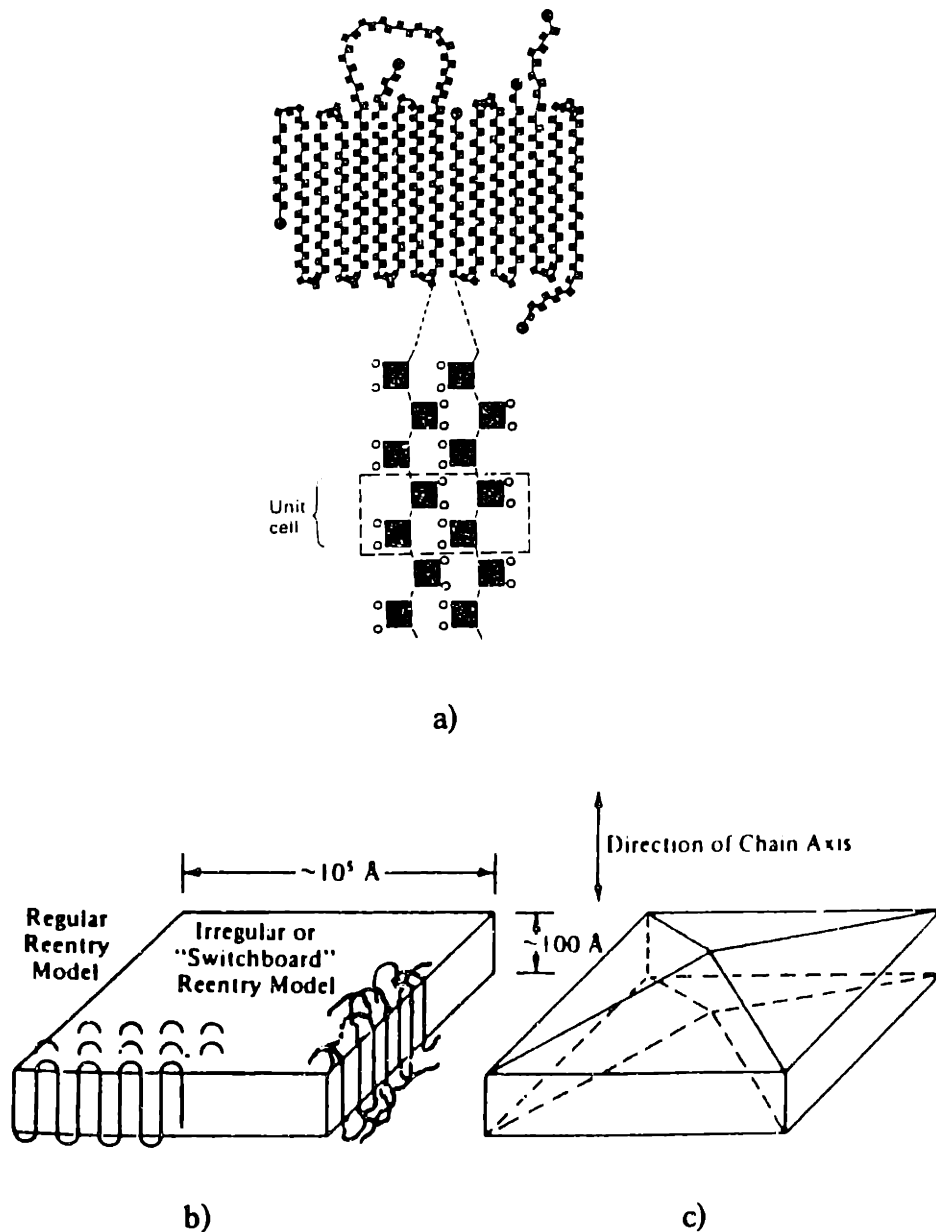


Figure 3 a) a chain-folded polymer crystal with a relatively simple unit cell b) a flat lamellae showing two concepts of chain re-entry c) a pyramidal lamellae [2, 12]

Unlike metals, which can be considered perfectly crystalline, polymers are seen to have a crystalline content of up to 98%, and most polymers considered crystalline are roughly 80% crystal. The chain folds are rarely perfectly even, and the tails of the molecules may mesh improperly and form dislocations. However, the crystallinity is good enough to diffract X-rays like a metal crystal and, as seen in Figure 3, a unit cell can be defined.

Not only do polymer chains arrange to form crystallites, but these crystallites often organize themselves into larger aggregates known as spherulites. These spherulites grow radially outward from a central point, forming crystals with spherical symmetry. Figure 4 shows the actual progression of spherulite growth.

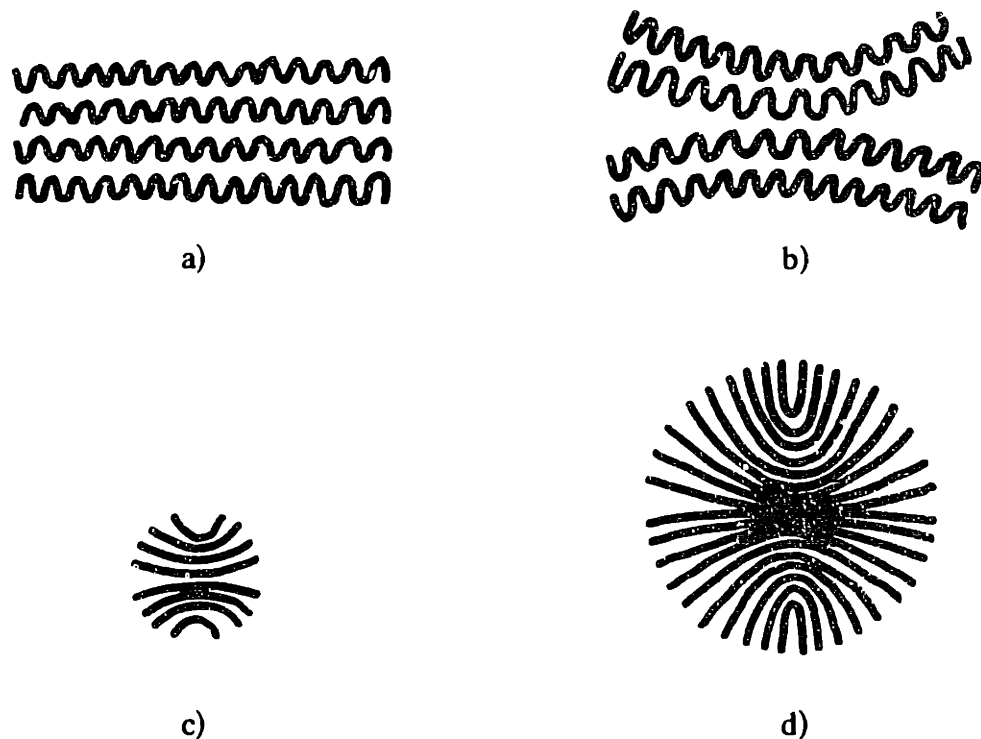


Figure 4

- a) A small bundle of growing crystallites.
- b) The growing bundle ends trap amorphous material between them, wedging them apart.
- c) More crystallites nucleate on the bundle, and they also splay out as they grow.
- d) The splaying continues until the crystallites bend back upon themselves. From this point, the spherulite grows radially until it impinges on others.

The spherical structure of spherulites make them in some ways similar to the grain structure found in metals. They are typically less than 10 micrometers in diameter and have a “Maltese cross” appearance between crossed polaroids. Because large spherulites contribute to brittleness in polymers, nucleating agents are often added or the polymer is shock cooled to promote smaller spherulites and reduce brittleness. Figure 5 shows the spherulite structure of a sample of isotactic polypropylene.

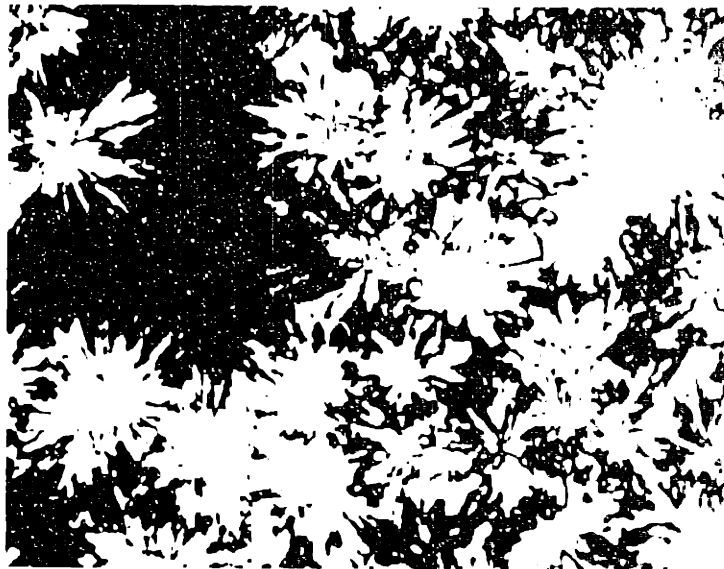


Figure 5 Isotactic polypropylene sample showing crystalline spherulites

Because crystallization results in more efficient and tighter packing of polymer chains, the crystallites will have a higher density. Also, because of this tight packing, crystallinity can significantly increase the strength and rigidity of a polymer. For example, increasing the percent crystallinity of polyethylene from 65% to 90% increases the tensile modulus from $0.97 - 2.6 \times 10^8$ Pa to $4.1 - 12.4 \times 10^8$ Pa, the tensile strength from $0.41 - 1.6 \times 10^7$ Pa to $2.1 - 3.8 \times 10^7$ Pa, and the flexural modulus from $0.34 - 4.1 \times 10^8$ Pa to $6.9 - 18 \times 10^8$ Pa [2].

1.5 Intent

Several models have been proposed in the last seven or eight years to predict the crystallinities of materials when subjected to a number of experiments. One of the most recent models was put forward by D.F. Baldwin and N.P. Suh of the Massachusetts Institute of Technology [3]. This gas sorption model proposes to predict the spatial distribution of gas and the crystalline morphology of the sample over time. The model is a complex, time-varying boundary problem.

The intent of this thesis is to solve a portion of the gas sorption model, the crystallinity model, through the application of molecular theory and the examination of experimental results. It is the further intent to compare the crystallinity predictions of the solved model to an independent set of experimental data in order to ascertain the solved model's accuracy.

Chapter 2 - Theoretical Models

2.1 Modeling Gas Sorption in Semi-Crystalline Polymers

D.F. Baldwin and N.P. Suh of the Massachusetts Institute of Technology introduced a gas sorption model in May of 1991 [3]. This model was designed to predict the spatial distribution of gas and the crystallizing morphology of a sample over time. The model was designed with the intent to predict the effects of gas sorption in semi-crystalline polymers in order to better understand the processes during which such polymers are foamed.

The sorption model is divided into two separate, but coupled, phenomenon: gas diffusion and polymer crystallization. The main modeling assumptions are that gas diffusion is governed by Fick's laws, and that polymers crystallize in a spherulite morphology. However, to apply the model more generally, these assumptions might have to be relaxed and the governing equations modified.

The coupled phenomenon of gas diffusion and polymer crystallization are modeled by using the following two part argument:

1) at high gas concentrations in the polymer matrix, the spacing between the long chain molecules increases, making it easier for the chains to move. This makes it easier for the polymer molecules to align for spherulite nucleation and growth. This increased spacing is modeled as a decrease in the activation energy.

2) as the spherulites grow, gas is pushed into the amorphous regions around the spherulites. This gas rejection occurs because the gas concentration within the spherulites is negligible.

The following two sections provide greater details on the gas diffusion model and the crystallization model.

2.2 Diffusion Model

The purpose of this section is to introduce familiarity with gas diffusion theory despite the fact that the diffusion model is dealt with only in a cursory manner in this thesis.

To model the diffusion characteristics of the gas-polymer system, Fick's first and second laws are used, and the model is restricted to analysis in two dimensions. Assuming negligible volume change in the polymer, gas concentration is governed by the following equation:

$$\frac{\delta c}{\delta t} = \left[\frac{\delta}{\delta x} \left(D \frac{\delta c}{\delta x} \right) + \frac{\delta}{\delta y} \left(D \frac{\delta c}{\delta y} \right) \right] \quad (1)$$

where c is the gas concentration in [$\text{cm}^3(\text{STP})/\text{cm}^3$], D is the gas-polymer system diffusivity in [cm^2/s], x and y are the spatial coordinate in [cm], and t is the diffusion time in [s]. Henry's law can be used to state the boundary conditions and the initial condition:

$$c(x, y, 0) = 0$$

$$c(x, -b, t) = K_s P_{\text{sat}}$$

$$\left(\frac{\delta c}{\delta y} \right)_{x, 0, t} = 0$$

$$c(\pm a, y, t) = K_s P_{\text{sat}} \quad (2)$$

where b is the half sheet thickness, a is the half sheet width, K_s is Henry's law solubility constant, and P_{sat} is the gas saturation pressure, which is typically held constant during sorption.

In the general case, gas-polymer diffusivity is a function of gas concentration and temperature. The polymer molecule mobility argument explains that increased polymer molecule mobility results in a lower activation energy for diffusion. An Arrhenius relation models the gas-polymer system diffusivity. The temperature and concentration dependence is modeled using a potential energy term, ΔU .

The diffusivity is given by:

$$D = D_0 \exp\left(\frac{\Delta E_D - \Delta U}{kT}\right) \quad (3)$$

where ΔE_D is the diffusion activation energy, ΔU is the potential energy change due to molecular spacing, k is Boltzmann's constant, and T is the gas-polymer crystallization temperature.

2.3 Crystallization Model

The key assumption in modeling the crystallization of the amorphous polymer matrix is that the crystalline morphology is spherulitic. Furthermore, it is assumed that the spherulitic nucleation rate is first order and given by the Arrhenius relation:

$$\dot{N} = \dot{N}_0 \exp\left(-\frac{\Delta E_N - \Delta U}{kT}\right) \exp(-\eta t) \quad (4)$$

where \dot{N}_0 is the initial spherulite nucleation density rate in [spherulites/cm³s], ΔE_N is the spherulite nucleation activation energy in [J], ΔU is the change in potential energy due to changes in molecular spacing, and η is the reciprocal spherulite nucleation time constant in [1/s].

The initial spherulite nucleation density rate can be considered a frequency term which determines the maximum number of spherulite nucleation sites possible, and a frequency factor for nuclei formation. The first exponential term represents the likelihood of forming those sites. The spherulite nucleation activation energy term is the amount of energy necessary to cause a spherulite to nucleate. The reciprocal spherulite nucleation time constant is the parameter which determines how quickly the spherulites will nucleate.

The spherulite growth rate can be modeled as constant. Since the molecule mobility argument holds for both spherulite nucleation and growth, the spherulite growth rate can be modeled by a first order Arrhenius relation:

$$\dot{r}_s = \dot{r}_{s0} \exp\left(-\frac{\Delta E_G - \Delta U}{kT}\right) \quad (5)$$

where \dot{r}_{s0} is a pre-exponential factor and ΔE_G is the activation energy for spherulite growth. The pre-exponential factor, \dot{r}_{s0} , can be considered a molecular jump frequency, or the likelihood that part of a polymer chain will align with the growing spherulite and take part in that spherulite's growth. The activation energy is the energy needed to allow the spherulite to grow. This linear spherulite growth rate has been verified for most polymers. Experimental evidence will be presented in Chapter 3.

2.4 Crystallinity Calculation

To predict the crystallinity of the material, three distinct regions must be considered: amorphous regions, growing or active spherulites, and inactive spherulites. The crystallinity can be predicted by taking the ratio of the crystal mass to the total sample mass. Assuming the sample is originally amorphous:

$$\chi = \frac{m_{as} + m_{is}}{\rho_a V_0} \quad (6)$$

where m_{as} is the mass of the active spherulites, m_{is} is the mass of the inactive spherulites, ρ_a is the density of the amorphous material, and V_0 is the initial volume of the sample.

In order to determine m_{as} and m_{is} , the following assumptions are made: 1) the reciprocal nucleation time constant, η , is large, such that spherulite nucleation can be considered instantaneous and uniform. It follows that the spherulite growth is also uniform; 2) the spherulites are randomly distributed throughout the polymer; 3) the center-to-center spacing between spherulites, r_a , is modeled following a normal distribution with mean μ and standard deviation σ ; and 4) spherulite growth ceases upon impingement. At

times during the solving of the crystallinity model, further simplifying assumptions will be made. For example, some calculations will assume regular packing of spherulites rather than random spacing.

The mass of active spherulites is defined in the model as the product of the volume of each active spherulite, the spherulite density, the total number of spherulites, and the fraction of spherulites that have not impinged:

$$m_{as} = \left[\frac{4}{3} \pi r_s^3 \right] \rho_c V_0 N \left(1 - \int_0^{2r_s} \frac{1}{\sqrt{2\pi}\sigma} \exp \left[- \frac{(r_a - \mu)^2}{2\sigma^2} \right] dr_a \right) \quad (7)$$

where ρ_c is the density of the spherulite region.

The mass of inactive spherulites is defined as the integral of the product of the density of a spherulite, the volume of the spherulites that impinge at a given spacing r_a , the total number of spherulites, and the fraction of spherulites that have impinged at r_a .

$$m_{is} = \int_0^{2r_s} \left[\frac{4}{3} \pi \left(\frac{r_a}{2} \right)^3 \right] \rho_c V_0 N \left[\frac{1}{\sqrt{2\pi}\sigma} \exp \left[- \frac{(r_a - \mu)^2}{2\sigma^2} \right] \right] dr_a \quad (8)$$

Using Equations 6, 7, and 8, the size, number, and distribution of the spherulites can be predicted as a function of time by integrating equations 4 and 5.

Chapter 3 - Solving the Crystallization Model

3.1 Calculating the Potential Energy Change

3.1.1 The Potential Energy Change at 120° C

At certain points during the solution of the crystallinity model the potential energy change at 120° C will need to be known. This term will be calculated in this section so that the value will be available when needed. It is first necessary to determine the molar volume of the polymer matrix.

A reference temperature, T_0 , and gas concentration, c_0 , are chosen at 25° C and 0.0 mol/cm³, respectively. Assuming the molar volume of the polymer matrix follows the continuum approximation, the local molar volume of the polymer matrix is given by:

$$V_m = (V_{mo} + \alpha(T - T_0)) \left[1 + \frac{c}{3BK_s} \right] \quad (9)$$

where V_{mo} is the molar volume at the reference conditions, α is the volumetric thermal expansion coefficient and B is the polymer matrix bulk modulus. Using Henry's law, the gas concentration is given by:

$$c = K_s P \quad (10)$$

where P is equal to gas pressure, the equation becomes

$$V_m = (V_{mo} + \alpha(T - T_0)) \left[1 + \frac{P}{3B} \right] \quad (11)$$

Plugging in values of 5.516×10^6 Pa for pressure (800 psi) and 120° C (393.15° K) for temperature, and using literature values for V_{mo} , α , and B , the calculation yields the molar volume.

$$V_{mo} = 144.5 \text{ cm}^3/\text{mol} \quad \alpha = 442 \times 10^{-4} \text{ cm}^3/\text{mol}^\circ\text{K} \quad B = 5.467 \times 10^9 \text{ Pa}$$

$$V_m = 161.9 \text{ cm}^3/\text{mol}$$

Using the molar volume we can predict the characteristic molecule-molecule interaction distance, R , under quasi-equilibrium conditions. In order to do this, the strophon theory developed by Yannas and Luise is used [15]. The strophon theory uses a first order approximation, which models polymer molecules as points with spherically symmetric potential fields. The characteristic interaction distance is given by:

$$R = 2 \left(\frac{3}{4\pi N_A} V_m \right)^{1/3} \quad (12)$$

where N_A is Avogadro's number. Plugging in the calculated molar volume allows R to be calculated. Plugging in the Van der Waals volume of $94.18 \text{ cm}^3/\text{mol}$ allows R_0 to be calculated where the Van der Waals volume is the theoretical volume occupied only by the PET molecules. These values are:

$$R = 8.0 \times 10^{-10} \text{ m}$$

$$R_0 = 6.7 \times 10^{-10} \text{ m}$$

By knowing the characteristic interaction distances, R and R_0 , the potential energy and change in potential energy of a two molecule system can be found by using Lennard-Jones 6-12 model:

$$U = - U_0 \left[\left(\frac{R_0}{R} \right)^{12} - 2 \left(\frac{R_0}{R} \right)^6 \right] \quad (13)$$

$$\Delta U = U - U_0 \quad (14)$$

where U_0 is the equilibrium potential energy of the system, which is estimated from the zero point enthalpy of PET. The energy terms are:

$$U_0 = - 10,000 \text{ J/mol}$$

$$U = - 5,711 \text{ J/mol}$$

$$\Delta U_{373} = 4,289 \text{ J/mol or } 7.12 \times 10^{-21} \text{ J}$$

3.1.2 The Potential Energy Change at 25° C

Because the change in potential energy due to increased molecular spacing, ΔU , is a term appearing in both Equation 4 and Equation 5, this value will be calculated before the spherulite growth rate and the spherulite nucleation rate are examined. To calculate ΔU , the molar volume at the testing conditions must first be found. Unlike the previous section, Equation 11 will not suffice to find the molar volume because of the choice of 25° C as reference temperature and because of the bulk material approach that equation takes. Therefore, another equation must be found which will accurately determine the molar volume at the testing conditions.

It is proposed that Equation 15 is a more appropriate way to find the molar volume because it deals with volume on a molecular scale. Qualitatively, Equation 15 suggests that molar volume of a CO₂ gas sorped sample is equivalent to the molar volume at the reference conditions, plus the volume of the CO₂ molecules present in the polymer matrix, minus the free volume which the CO₂ molecules have filled.

$$V_m = V_{mo} + (c N_A V_{CO2} V_{mo} - (V_{mo} - V_w)) \quad (15)$$

where c is the CO₂ gas concentration, N_A is Avogadro's number, V_{CO2} is the volume of a CO₂ molecule, and V_w is the Van der Waals volume at the reference conditions.

Substituting $c = K_s P$ and plugging in the known values for the other constants gives the molar volume.

$$V_{mo} = 144.5 \text{ cm}^3/\text{mol}$$

$$c = K_s P = 0.538 \text{ cm}^3\text{STP}/\text{cm}^3\text{bar} * 800 \text{ PSI} = 0.665 \text{ mol}/\text{cm}^3$$

$$N_A = 6.02 \times 10^{23} \text{ molecules}/\text{mol}$$

$$V_{CO2} = 5.17 \times 10^{-24} \text{ cm}^3$$

$$V_w = 94.18 \text{ cm}^3/\text{mol}$$

$$V_m = 393.3 \text{ cm}^3/\text{mol}$$

Once the molar volume is known, the characteristic interaction distances can be found as in Section 3.1.1 and are:

$$R = 1.08 \times 10^{-9} \text{ m}$$

$$R_0 = 6.7 \times 10^{-10} \text{ m}$$

The potential energy and change in potential energy can also be calculated in the same manner as in Section 3.1.1.

$$U_0 = - 10,000 \text{ J/mol}$$

$$U = - 1,108 \text{ J/mol}$$

$$\Delta U_{298} = 8,892 \text{ J/mol or } 1.48 \times 10^{-20} \text{ J}$$

3.2 Finding the Spherulite Growth Rate

In order to find the spherulite growth rate, two separate approaches are taken. The first approach is to analyze crystallization data on PET and to extract out the information needed to complete the model equations. The second approach involves examining the theory behind the growth rate formula and attempting to define the constants in terms which can be easily calculated.

3.2.1 Experimental Analysis

S.A. Jabarin reports observed values for spherulite growth rates of PET at various temperatures [7]. By reducing Equation 5 in the following manner:

$$\dot{r}_s = \dot{r}_{s0} \exp\left(-\frac{\Delta E_G - \Delta U}{kT}\right) \quad (5)$$

$$\ln \dot{r}_s = \ln \dot{r}_{s0} - \frac{\Delta E_G - \Delta U}{kT}$$

$$\ln \dot{r}_s = (\Delta E_G - \Delta U) * \left(-\frac{1}{kT}\right) + \ln \dot{r}_{s0} \quad (16)$$

it is possible to graph the natural logarithm of the spherulite growth rate, \dot{r}_s , against the negative reciprocal of the temperature times Planck's constant. By recognizing that Equation 16 is of the form:

$$y = m * x + b \quad (17)$$

the molecular jump frequency, \dot{r}_{s0} , can be calculated from the y-intercept, and the activation energy term, $(\Delta E_G - \Delta U)$, can be calculated from the slope of the line. Using Jabarin's values in Table 1 to form the graph in Figure 6, provides the following results using standard linear regression techniques:

$$\dot{r}_{s0} = 4.02 \times 10^8 \text{ m/s}$$

$$(\Delta E_G - \Delta U) = 1.61 \times 10^{-19} \text{ J}$$

Table 1. Spherulite Growth Rate, \dot{r}_s , at Various Temperatures	
Temp. ° C	\dot{r}_s , μ /sec
110	0.6×10^{-3}
115	1.0×10^{-3}
120	2.5×10^{-3}
125	4.2×10^{-3}
130	8.7×10^{-3}

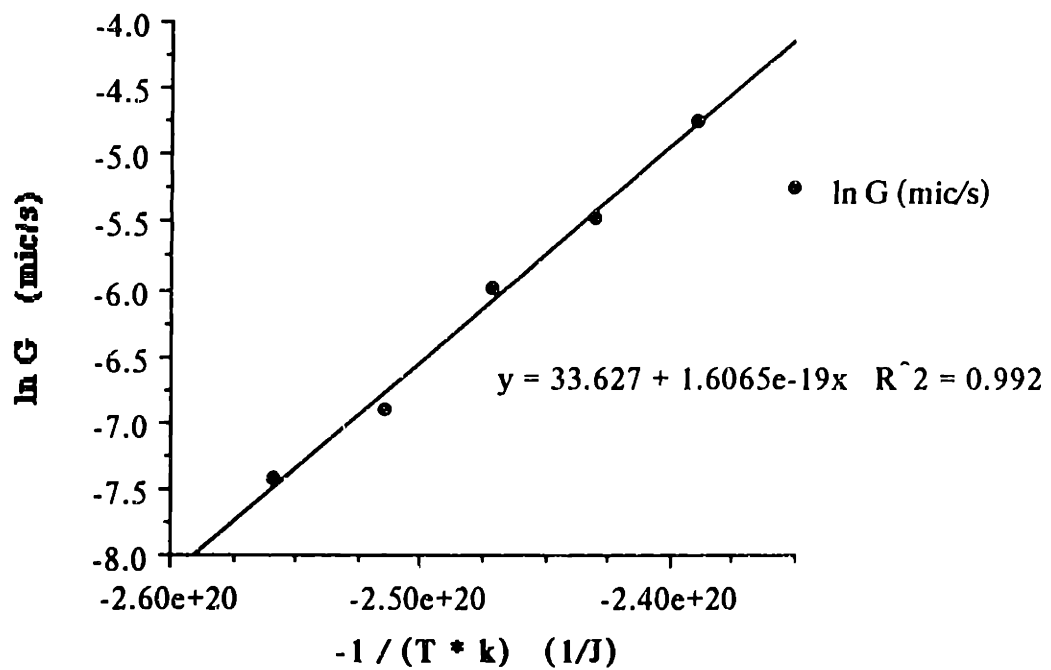


Figure 6 Determining spherulite growth rate and the activation energy term by experiment

In order to find the activation energy for spherulite growth, ΔE_G , the potential energy term from Section 3.1.1 is added to the activation energy quantity. This yields an activation energy of:

$$\Delta E_G = 1.68 \times 10^{-19} \text{ J}$$

The spherulite growth rate, \dot{r}_s , can be found by inserting the values for \dot{r}_{s0} , ΔE_G , and ΔU for 25° C (found in Section 3.1.2) into Equation 5. This substitution yields the spherulite growth rate for crystallization at 25° C and 800 psi:

$$\dot{r}_s = 2.7 \times 10^{-8} \text{ m/s}$$

3.2.2 Theoretical Analysis

J.D. Muzzy, et al, assume that spherulites pack in a face-centered cubic (FCC) structure [11]. This is equivalent to assuming that all neighboring spherulite nuclei are equidistant. While this is probably not the case, it can be said that the center-to-center distance in the FCC structure should correspond to the average distance between nuclei in a random structure. By further assuming no induction time, all of the spherulites at a given penetration distance must impinge at the same time.

For our model, which assumes regular chain folding at 25° C:

$$\dot{r}_s = \dot{r}_{s0} \exp\left(-\frac{\Delta E_G - \Delta U}{kT}\right) \quad (5)$$

where \dot{r}_s is the radial growth rate of the spherulites. For this model, \dot{r}_{s0} represents a molecular jump frequency:

$$\dot{r}_{s0} = \frac{a_0 kT}{h} \quad (18)$$

where a_0 is the width of the triclinic PET cell (see Figure 7), k is Planck's constant, T is the crystallization temperature, and h is Boltzmann's constant. The molecular jump frequency is the likelihood that a section of polymer chain will "snap" into place and cause spherulite growth.

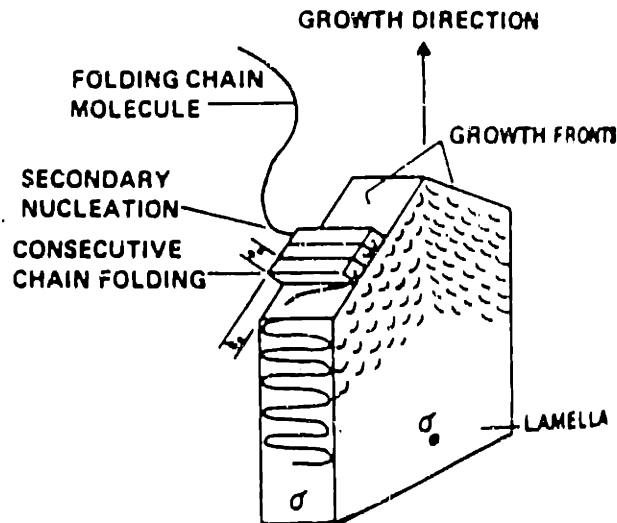


Figure 7 Model of lamellar growth front assuming regular chain folding.
 $a_0 = 0.448 \pm 0.05 \text{ nm}$ [11]

Inserting accepted values for a_0 , k , h , and setting the temperature at 25° C, the calculation of the molecular jump frequency yields:

$$\dot{r}_{s0} = 2.78 \times 10^3 \text{ m/s}$$

To find a value for ΔE_G , the activation energy for spherulite growth, it is necessary to turn to a combination of theory and experimental data. As in Section 3.1.1, Equation 5 can be reduced to a form in which $(\Delta E_G - \Delta U)$ can be found:

$$\ln\left(\frac{\dot{r}_s}{\dot{r}_{s0}}\right) = (\Delta E_G - \Delta U) * \left(-\frac{1}{kT}\right) \quad (19)$$

Graphing, as in Section 3.2.1, yields a value for the activation energy term:

$$(\Delta E_G - \Delta U) = 1.61 \times 10^{-19} \text{ J}$$

Because only the molecular jump frequency changed, only the y-intercept of the graph is affected, and the activation energy term, defined by the slope, remains the same as in Section 3.2.1.

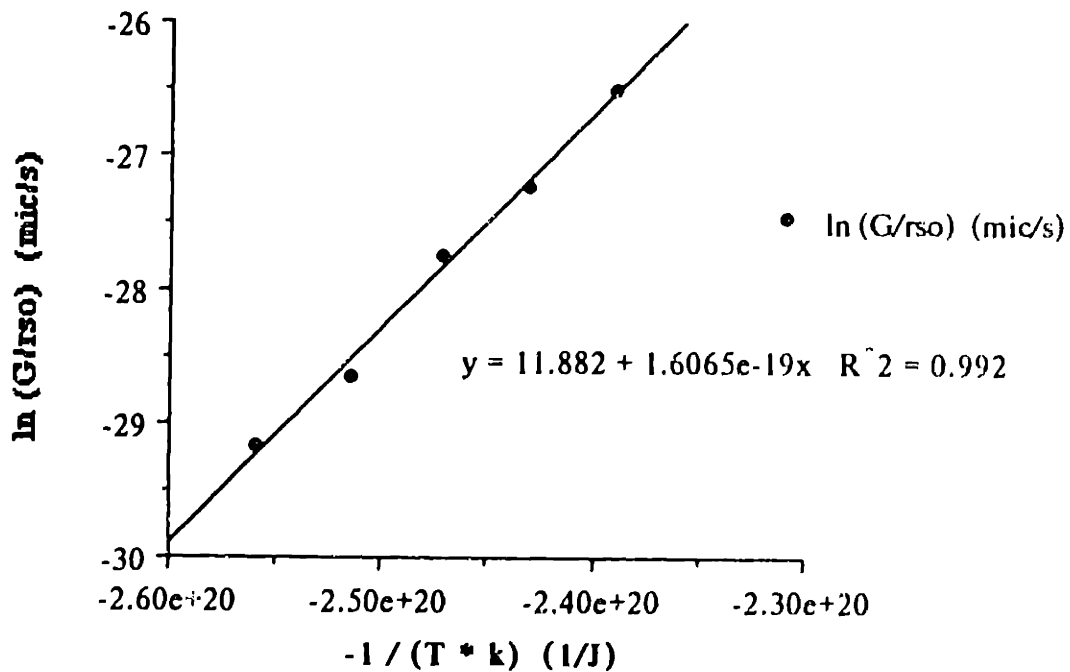


Figure 8 Determining spherulite growth rate and the activation energy term

The activation energy is found by adding the potential energy term of Section 3.1.1 as before:

$$\Delta E_G = 1.68 \times 10^{-19} \text{ J}$$

The spherulite growth rate, \dot{r}_s , can be found by inserting the values for \dot{r}_{sG} , ΔE_G , and ΔU as before:

$$\dot{r}_s = 1.87 \times 10^{-13} \text{ J}$$

It should be noted that this value for the spherulite growth rate is substantially smaller than that predicted by experimental analysis. This is due to the assumption that the width of the triclinic cell, multiplied by the frequency factor, is a true determinant of the spherulite growth rate.

3.3 Finding the Spherulite Nucleation Rate

As with the determination of the spherulite growth rate, the analysis of equation theory and experimental data is necessary to find the spherulite nucleation rate. This portion of the model is more strongly guided by the theoretical aspects of the gas sorption model, with the experimental data lending credence and providing qualitative results.

3.3.1 Calculating the Initial Spherulite Nucleation Density Rate

Similar to the theoretical calculation for the molecular jump frequency, r_{s0} , the initial spherulite nucleation density rate, \dot{N}_0 , can be expressed as a spherulite nucleation frequency:

$$\dot{N}_0 = \frac{n_s k T}{h} \quad (20)$$

where n_s is the maximum number of nucleation sites per cubic centimeter, k is Planck's constant, T is the crystallization temperature, and h is Boltzmann's constant. The maximum number of nucleation sites per cubic centimeter is equal to the total number of polymer molecules per mole and can be calculated from the following equation:

$$n_s = \frac{N_A \rho_a}{MW} \quad (21)$$

where N_A is Avogadro's number, ρ_a is the density of amorphous PET ($\rho_a = 1.33 \text{ g/cm}^3$), and MW is the molecular weight of the PET used ($MW = 38,000 \text{ g/mol}$). By calculation:

$$n_s = 2.11 \times 10^{25} \text{ sites/m}^3, \text{ and thus:}$$

$$\dot{N}_0 = 1.31 \times 10^{38} \text{ sites/m}^3\text{s}$$

3.3.2 Modeling the Reciprocal Nucleation Time Constant

The reciprocal nucleation time constant, η , is the term in Equation 4 which makes the spherulite nucleation rate an exponential function. The addition of a time constant term to this equation causes more difficulty in solving for the spherulite nucleation rate than was present in the solving of the spherulite growth rate. In fact, even with a large amount of experimental data from the past decade on crystallization of PET, there is not enough information found at present to solve for the remaining three variables in the nucleation equation directly. Because the reciprocal time constant can be taken to a limit without severe damage to the model integrity, this term will be simplified.

By assuming that η goes to infinity, the time exponential term becomes unity. Effectively, Equation 4 becomes similar in form to that of the spherulite growth rate equation:

$$\dot{N} = N_0 \exp\left(-\frac{\Delta E_N - \Delta U}{kT}\right) \quad (22)$$

This assumption models nucleation as an impulse. All spherulites nucleate at the same point in time and grow from that moment until impingement, which will occur at different times for all spherulites, due to their random spacing. Because one of the three variable terms has been eliminated through this modelling assumption, the remaining two terms can be computed from crystallization data

3.3.3 Applying the Spherulite Nucleation Rate

As with the spherulite growth rate, a somewhat roundabout route must be taken in order to define all of the constants in Equation 4. Because no data is available on the activation energy term, the spherulite nucleation rate will be calculated from experimental data.

Assuming impingement has not occurred, the polymer crystallinity can be stated by the following equation:

$$\chi = \frac{m_{as}}{m_T} \quad (23)$$

where χ is crystallinity, m_{as} is the mass of the active spherulites, and m_T is the total polymer mass. This equation can be expanded as follows:

$$\chi = \frac{4 \rho_c \pi (r_s * t)^3}{3 \rho_a} * N \quad (24)$$

where ρ_c is the crystalline density of the polymer, ρ_a is the amorphous density of the polymer, and N is the integral of the spherulite nucleation rate.

Crystallinity, χ , can be determined for PET by analyzing a set of Depolarized Light Intensity (DLI) experiments performed by S.A. Jabarin [7]. These experiment yielded crystallinity isotherms for PET samples at various temperatures. From these isotherms, it is possible to determine the Avrami constants for PET.

The Avrami equation is:

$$\chi(t) = 1 - \exp[- Kt^n] \quad (25)$$

where K and n are the Avrami constants. With the constants for a material, it is possible to calculate the crystallinity over time. Figure 9 is a graph of the crystallinity isotherms found by Jabarin. The vertical axis is in terms of $\ln(-\ln\Theta_a)$, where Θ_a is the depolarized light

intensity, and the horizontal axis is in terms of $\ln(t - t_0)$. Following an isotherm to its y-intercept will yield the constant K, and the slope of the isotherm corresponds to the exponent n. Table 2 summarizes the analysis of the graph.

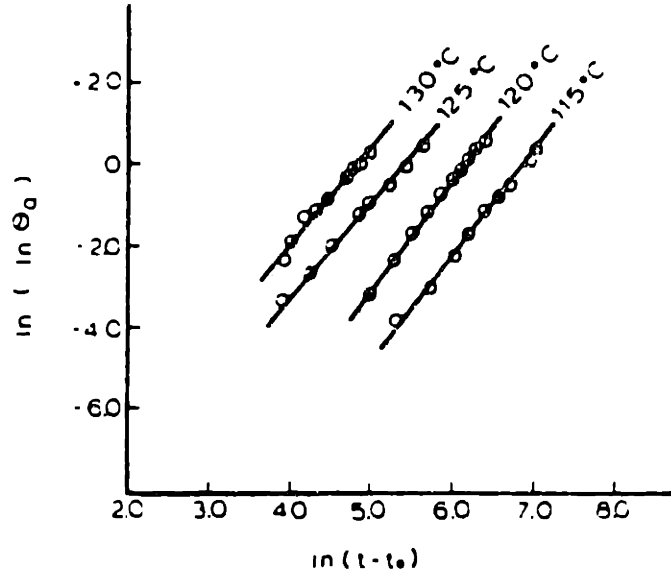


Figure 9 Avrami plot of crystallization of PET at various temperatures [7]

Table 2. Avrami Constants of PET at Various Temperatures		
Temp. °C	n	K
115	2.6	1.9×10^{-8}
120	2.6	6.8×10^{-8}
125	2.3	3.3×10^{-6}
130	2.3	1.0×10^{-5}

Returning to Equation 24, the crystallinity can be plotted against the density ratio term, Equation 24b, when the Avrami constants are known (see Figure 10).

$$\text{d.r.t.} = \frac{4 \rho_c \pi (\bar{r}_s * t)^3}{3 \rho_a}$$

By doing so, the slope of the linear region of the graphs, one for each temperature, will equal N . Because the reciprocal spherulite nucleation time constant η was taken to infinity, causing the exponential time term to vanish, the values taken for N are equivalent to \dot{N} , less an integration constant, which is assumed to be zero. The values for \dot{N} (and N), taken from the graphs in Figure 9, are summarized in Table 3.

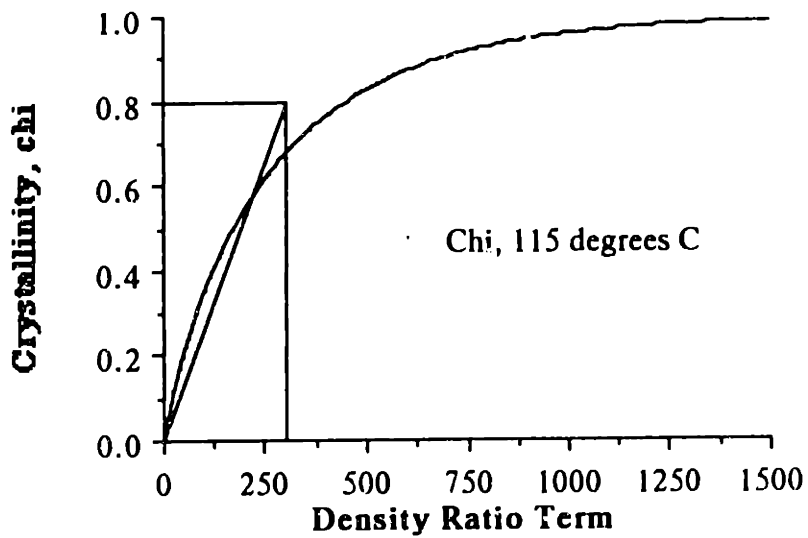


Figure 10a Determining the spherulite nucleation rate from crystallinity and density terms.

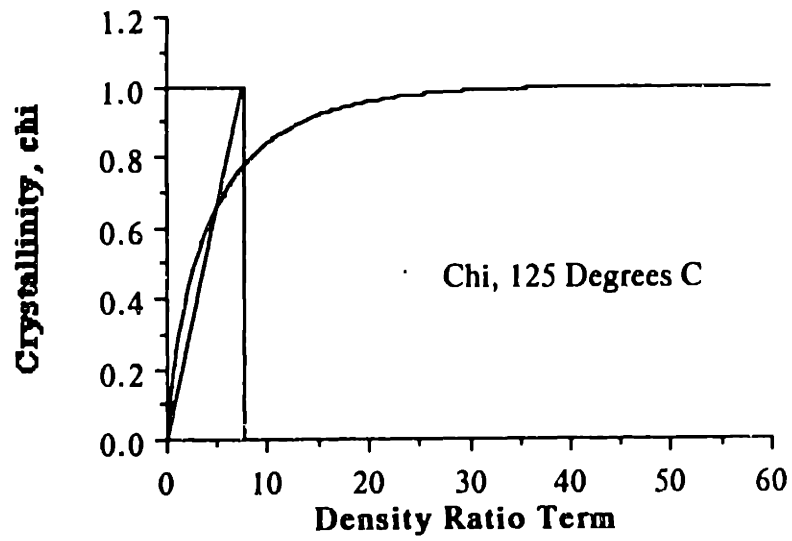
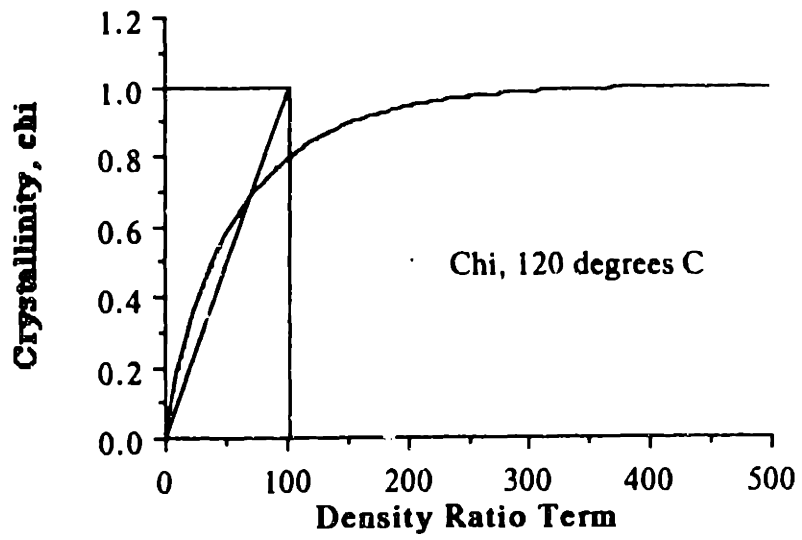


Figure 10b,c Determining the spherulite nucleation rate from crystallinity and density terms.

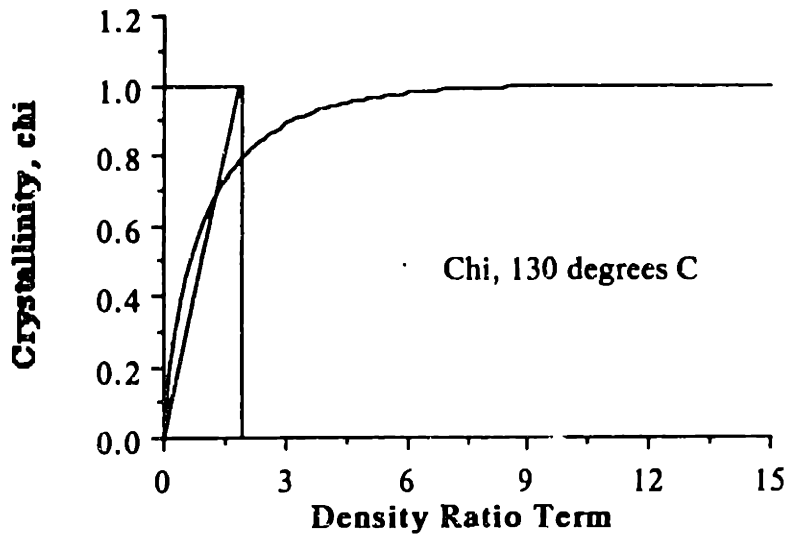


Figure 10d Determining the spherulite nucleation rate from crystallinity and density terms.

Table 3. Spherulite Nucleation Rate, \dot{N} , for Various Temperatures	
Temp. °C	\dot{N} , spherulites/m ³ s
115	2.6×10^{15}
120	10×10^{15}
125	125×10^{15}
130	555×10^{15}

Jabarin suggests using the method of Van Antwerpen and Van Krevelen, who used the following equation to calculate the nucleation density when crystallizing PET:

$$N = \frac{1}{\frac{4}{3} \pi R_{\max}^3} \quad (26)$$

where R_{\max} is the maximum spherulite radius. Jabarin lists this radius as 2.2 micrometers based on experimental measurements. This radius yields a value for N of $22 \times 10^{15} \text{ m}^{-3}$. This value will be used instead of any of the calculated values because of the consistency with which this value has been reported. The calculated values serve to check the model theory and simplifications.

3.3.4 Finding the Spherulite Nucleation Activation Energy

According to the crystallization model:

$$\dot{N} = \dot{N}_0 \exp\left[-\frac{\Delta E_N - \Delta U}{kT}\right] \exp(-\eta t) \quad (4)$$

Because it has been assumed that η goes to infinity, the exponential time term disappears. Upon rearranging the equation, the spherulite nucleation activation energy term can be solved:

$$(\Delta E_N - \Delta U) = -kT * \ln\left(\frac{\dot{N}}{\dot{N}_0}\right) \quad (27)$$

Both \dot{N} and \dot{N}_0 have been determined by theory, and upon plugging them into Equation 27, the activation energy term is found to be:

$$(\Delta E_N - \Delta U) = 2.72 \times 10^{-19} \text{ J}$$

As with the activation energy for spherulite growth, the potential energy from Section 3.1.1 is added to find:

$$\Delta E_N = 2.79 \times 10^{-19} \text{ J}$$

3.3.5 Solving for the Spherulite Nucleation Rate

Now that all of the constants for Equation 4 have been solved, they can be substituted in to find the spherulite nucleation rate, \dot{N} , at the desired experimental conditions. The initial spherulite nucleation density rate, the spherulite nucleation activation energy, and the potential energy change for 25° C and 800 PSI are placed in the equation to yield the spherulite nucleation rate:

$$\dot{N} = 1.70 \times 10^{10} \text{ spherulites/m}^3\text{s}$$

3.4 Analytically Predicting the Mass Fraction of Crystalline Material

Having solved Equations 4 and 5, it only remains to plug these values into Equations 6, 7, and 8, along with the value for crystalline density, and to choose an appropriate mean, μ , and standard deviation, σ . In section 3.3.3, Jabarin's value for the maximum spherulite radius was given as 2.2 micrometers. This value is chosen to be the mean. The standard deviation is chosen to be 1 micrometer.

The integrals of Equations 7 and 8 were solved by a numerical integration program, MathCad. The calculation sheet is in Appendix 3. The crystallinity vs. saturation time graph is shown below in Figure 11. Of particular note is the time range, 0 to 115 seconds, and the maximum crystallinity, 24%. The value used in the calculations for \dot{r}_s , the spherulite growth rate, is that calculated in Section 3.2.1. The value used for \dot{N} , the spherulite nucleation rate, is that given by Jabarin in Section 3.3.3.

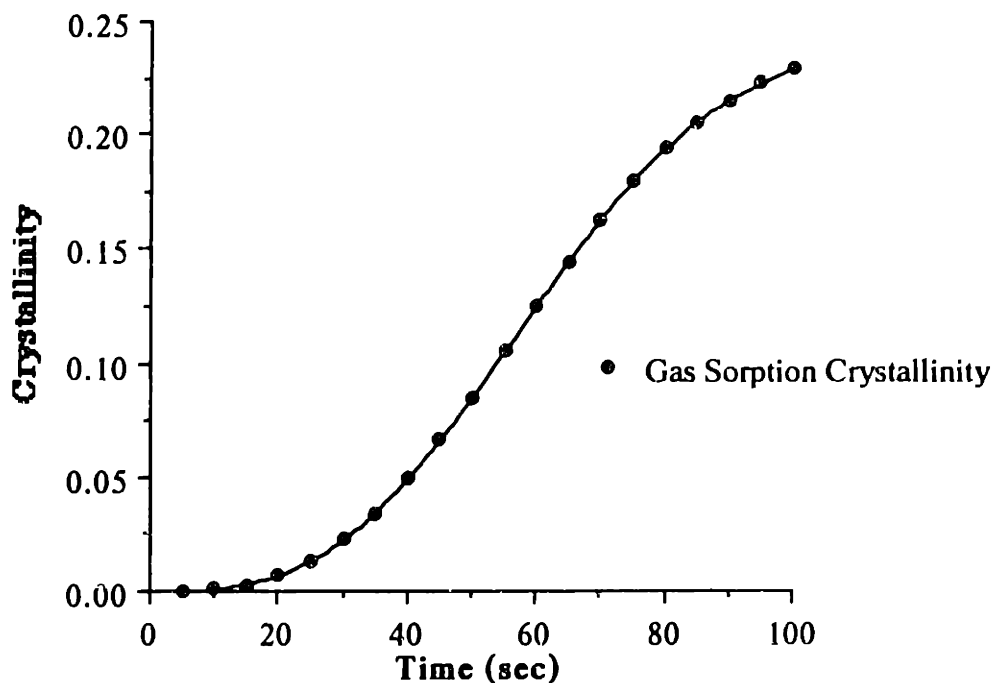


Figure 11 Gas sorption model crystallinity vs. time plot

Chapter 4 - Experimental Method and Results

4.1 Procedure

To verify the predictive capacity of the crystallinity model, several crystallization experiments were performed. These experiments were gas-sorptions of PET at a standard pressure of 800 psig and of varying saturation times. All experiments were performed on Kodak PET 9921 film of roughly 0.028 inches thickness. All experiments were run at room temperature of 25° C.

Each sample was weighed before testing, and the thickness was measured. The samples were placed in a pressure chamber for periods of time ranging from 5 to 380 hours. Because the critical period of crystallization was expected to be in the range of 10 to 30 hours, several samples were saturated for those periods of time.

When the saturation period was over, the samples were collected and weighed within 2.5 minutes of the pressure release. This was to ensure an accurate final weight measure to observe the percent weight gain of the material.

The samples were analyzed by differential scanning calorimeter to determine the extent to which each was crystallized. An unmodified sample and a thermally crystallized sample were also analyzed. A DSC sample was taken of an Indium sample during each period of analysis in order to find the baseline of the DSC runs. The crystallization data was compiled and plotted as a whole against time.

4.2 Apparatus

The gas sorption chamber was simply a steel pressure vessel sealed by an o-ring and secured by heavy duty bolts and an impact wrench. One valve piped CO₂ into the chamber, and a release valve bled off the pressure when the chamber was to be opened.

The samples were analyzed on a Perkin-Elmer DSC7. The sample scan speed was set to 20° C/min, and the samples were tested between the temperatures of 20° C and 300° C.

4.3 Results

A typical plot of heat flow vs. temperature for a PET sample having undergone DSC analysis is shown below in Figure 12. The sample was saturated for 30 hours, at the standard pressure of 800 psig and room temperature of 25° C. The initial weight was 0.51630 g and the weight after gas sorption was 0.55612 g. The sample shows a weight gain of 7.7%. To calculate crystallinity, it is necessary to study the peaks shown in the graph.

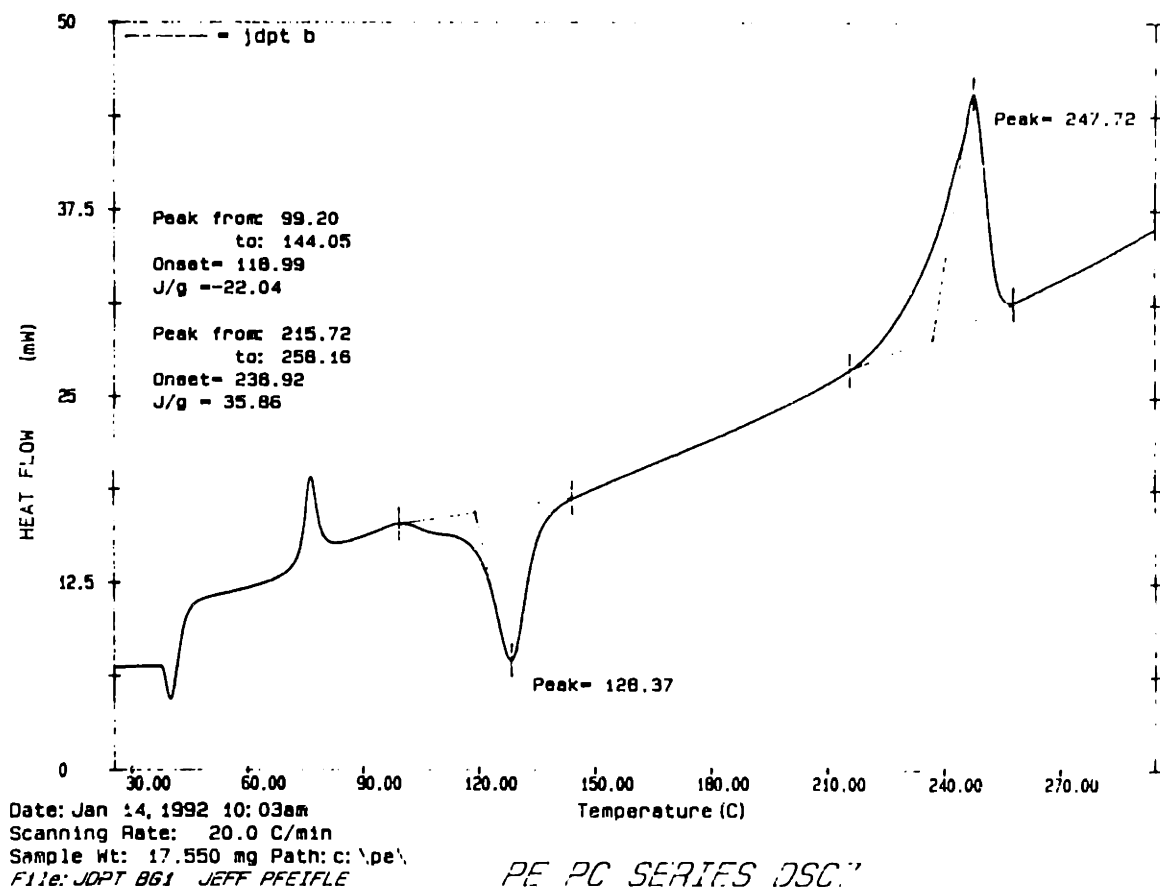


Figure 12 DSC thermogram for PET sample saturated for 30 hours at 800 psig and 25° C.

There are two major peaks shown in Figure 12. The peak at the far right is the melt endotherm. The negative peak, or valley, is the crystallization exotherm. To calculate the degree of crystallinity in a sample, it is necessary to subtract the area of the crystallization

exotherm from the area of the melt endotherm, multiply by a baseline correction factor, and divide by the area value of a 100% crystal sample, as shown in Equation 28:

$$\chi = f \frac{P_m - P_c}{P_T} \quad (28)$$

where f is the correction factor, P_m is the area under the melt endotherm, P_c is the area "under" the crystallization exotherm, and P_T is the total possible area.

The correction factor, f , is calculated by dividing the experimental results of a baseline Indium run by the expected values. For all three testing periods, $f = 0.988$. P_T is tabulated as 125.58 J/g for PET. The calculated crystallinities and weight gains for all of the samples are calculated in Table 4, and crystallinity vs. saturation time is graphed in Figure 13 on the following page. The DSC graphs are in Appendix D.

Table 4. Crystallinity and Weight Gain Calculations for PET Samples			
I.D.	Sat. Time (hrs)	χ (%)	Wt. Gain (%)
um	0.00	4.7	
a	30.00	11.1	7.88
b	30.00	10.9	7.71
c	30.00	10.6	7.85
d	30.00	8.6	5.66
e	10.00	5.2	5.45
f	10.00	4.7	5.23
g	10.00	3.7	5.23
h	10.00	5.5	5.17
2	380.70	29.5	5.76
3	376.33	30.9	5.80
4	45.50	28.7	7.88
5	116.50	30.4	6.57
6	5.42	5.4	4.43
7	48.00	28.0	7.06
8	20.00	11.9	7.51
9	24.00	11.5	7.85
12	94.33	30.0	6.38

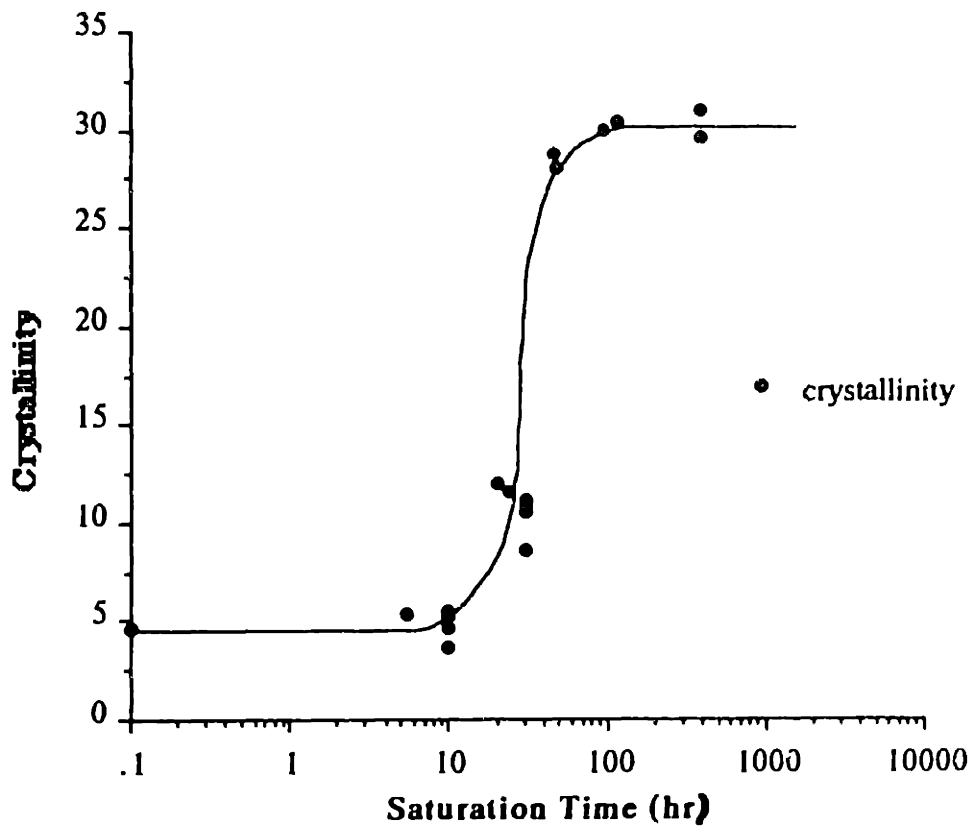


Figure 13 Crystallinity vs. Saturation Time for Kodak PET 9921

Chapter 5 - Verifying Model Prediction

5.1 Comparison of Model and Experimental Results

Figure 14 is a graph which plots the experimental results of crystallinity against saturation time and the results predicted by the gas sorption model. As can be seen, the shape of the two graphs are similar. The difference in time scale is dealt with below.

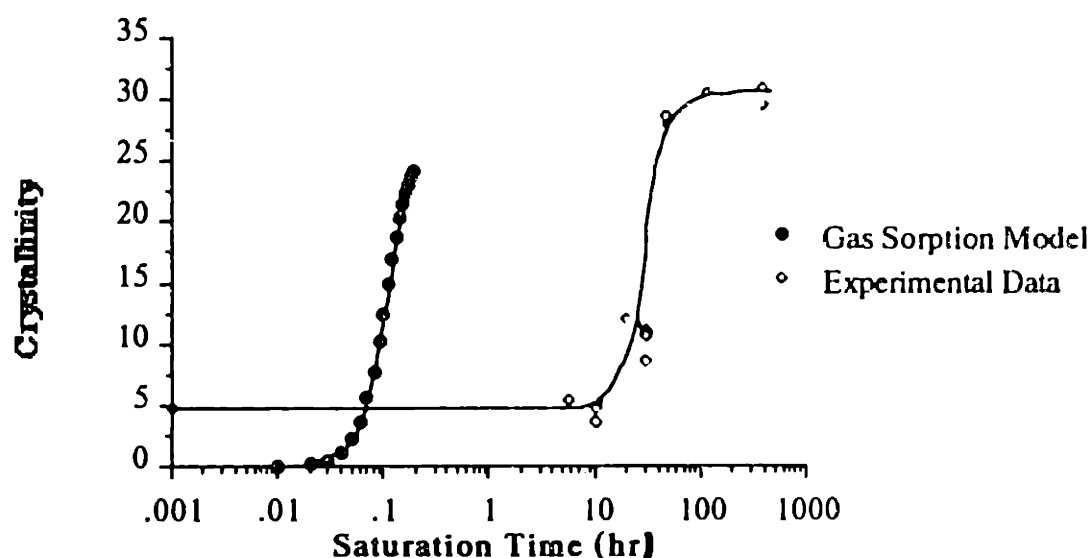


Figure 14 Gas sorption model predicted crystallinity plot and that found experimentally

Figure 14 shows a small difference, about 5%, in the crystallinity predicted by the gas sorption model and the crystallinity found experimentally. Some of this may be due to the DSC7 used to analyze the experimental data. As can be seen in Table 4 and in Figures 13 and 14, the DSC7 predicted 4.7% crystallinity in the unmodified amorphous sample, which should have been 0.0% crystalline. This error, which may result from the DSC7 or from the operator, could have been propagated throughout the experimental analysis, causing a vertical shift in the experimental data graph of roughly 5%.

The time shift is due to the value used for \dot{r} in the gas sorption model. This value, the spherulite growth rate, is too large for that observed experimentally. A truer rate would be an order of magnitude or two lower. This discrepancy in growth rate is introduced into the model through the calculation of r_{50} and DEG by experimental means. However, without more data on CO₂ gas sorption at 25° C, a more accurate calculation can not be performed.

5.2 Discussion

In Section 5.1, the lack of data on gas sorption of PET at room temperature was briefly mentioned. Because of this lack of data, interpolation from data on gas sorption at higher temperatures, approximately 120° C, becomes necessary. Unfortunately, such interpolation can not provide the accuracy which is necessary in some of the equations of the gas sorption model. Therefore, attempting to verify the experimental data with theoretical rationale can provide a guide to the accuracy of the resulting equations.

Dealing with the potential energy changes due to the changes in molecular spacing is not easy. The uncertainty as to the molar volume of the PET after gas sorption makes this determination very difficult. Without a way to accurately determine this volume, only rough estimates can be found through theory.

The equations used to find the material crystallinity employ a mean and standard deviation. The choice of these values can alter the predicted crystallinity curve and so care must be taken when choosing these values. For this reason, these values were chosen conservatively.

The true value of the reciprocal spherulite nucleation time constant, η , may alter the aspect of the crystallinity curve with time. Because a constant value was used for N in this thesis, the effect of η is not known.

5.3 Conclusions

Despite the lack of data for the gas sorption of PET at room temperature, the accuracy with which the model predicts the general characteristics of the crystallinity curve is impressive and definitely warrants the further investigation of the proposed model.

Future work in determining the value of and effects of η , as well as examining the molar volume of the gas saturated material, can provide much needed insight in the analysis of the model. Experimental data on gas sorption at room temperature can provide the necessary information to more accurately define the values found in this thesis.

When the gas sorption model is defined to a better degree of accuracy, it will be able to provide much insight into the complexities of the gas sorption of semi-crystalline polymers and provide more opportunity for the application of materials such as microcellular foamed plastics.

Appendix A - Nomenclature

c	gas concentration
D	gas-polymer diffusivity
x, y	spatial coordinates
b	half sheet thickness
K_s	Henry's law solubility constant
P_{sat}	gas saturation pressure
ΔE_D	diffusion activation energy
ΔU	potential energy change
k	Boltzmann's constant
T	temperature
\dot{N}	spherulite nucleation rate
\dot{N}_0	initial spherulite nucleation density rate
ΔE_N	spherulite nucleation activation energy
η	reciprocal spherulite nucleation time constant
t	time
\dot{r}_s	spherulite growth rate
\dot{r}_{s0}	molecular jump frequency
ΔE_G	activation energy for spherulite growth
χ	crystallinity
m_{as}	mass of active spherulites
m_{is}	mass of inactive spherulites
ρ_a	density of amorphous material
ρ_c	density of crystalline material
μ	mean value
σ	standard deviation
B	polymer matrix bulk modulus
α	volumetric thermal expansion coefficient
P	pressure
N_A	Avogadro's number
R	characteristic molecule interaction distance
V	volume

Appendix B - Important Numbers

$k = 1.38 \times 10^{-23} \text{ J/}^\circ\text{K}$	Planck's constant
$h = 6.63 \times 10^{-34} \text{ Js}$	Boltzmann's constant
$N_A = 6.02 \times 10^{23} / \text{mol}$	Avogadro's number
$MW = 38,000 \text{ g/mol}$	Molecular weight of PET samples
$IV = 0.83$	Inherent Viscosity of PET samples
$\rho_a = 1.33 \text{ g/cm}^3$	Amorphous density of PET
$\rho_c = 1.501 \text{ g/cm}^3$	Crystalline density of PET
$T_c = 298.15^\circ \text{ K}$	Temperature of crystallization
$U_0 = -10,000 \text{ J/mol}$	Equilibrium potential energy
$V_w = 94.18 \text{ cm}^3/\text{mol}$	Van der Waals volume
$V_{mo} = 144.5 \text{ cm}^3/\text{mol}$	Molar volume at 25° C
$\alpha_g = 442 \times 10^{-4} \text{ cm}^3/\text{mol}^\circ\text{K}$	Volumetric thermal expansion coefficient
$B = 5.467 \times 10^9 \text{ N/m}^2$	Polymer matrix bulk modulus
$K_s = 0.538 \text{ cm}^3 \text{ STP/cm}^3 \text{ bar}$	Henry's law solubility constant
$P_s = 800 \text{ psig}$	Saturation pressure

Appendix C - MathCad Calculation Sheet

$$N = 22 \cdot 10^{15} \quad \rho_{\alpha} = 1.33$$

$$V_0 = 1 \quad \rho_{\chi} = 1.501$$

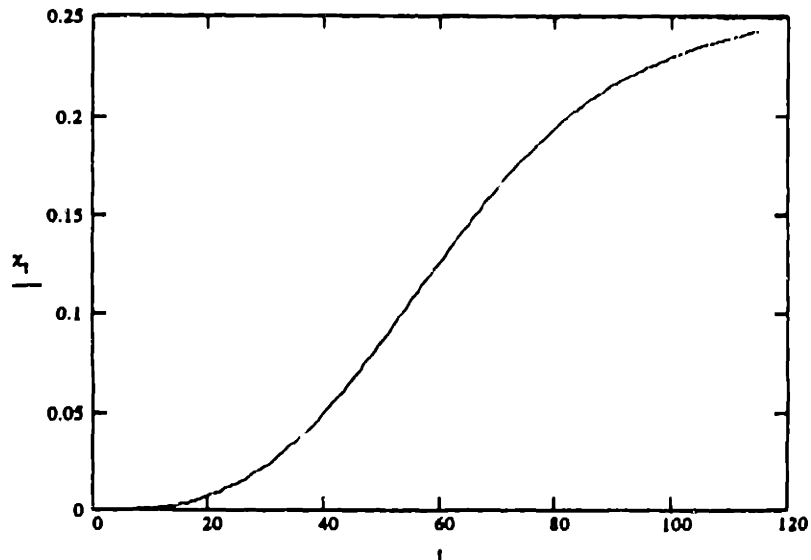
$$t = 1.115 \quad \mu = 2.2 \cdot 10^{-6}$$

$$r_t = 2.07 \cdot 10^{-8} \cdot t \quad \sigma = 1.0 \cdot 10^{-6}$$

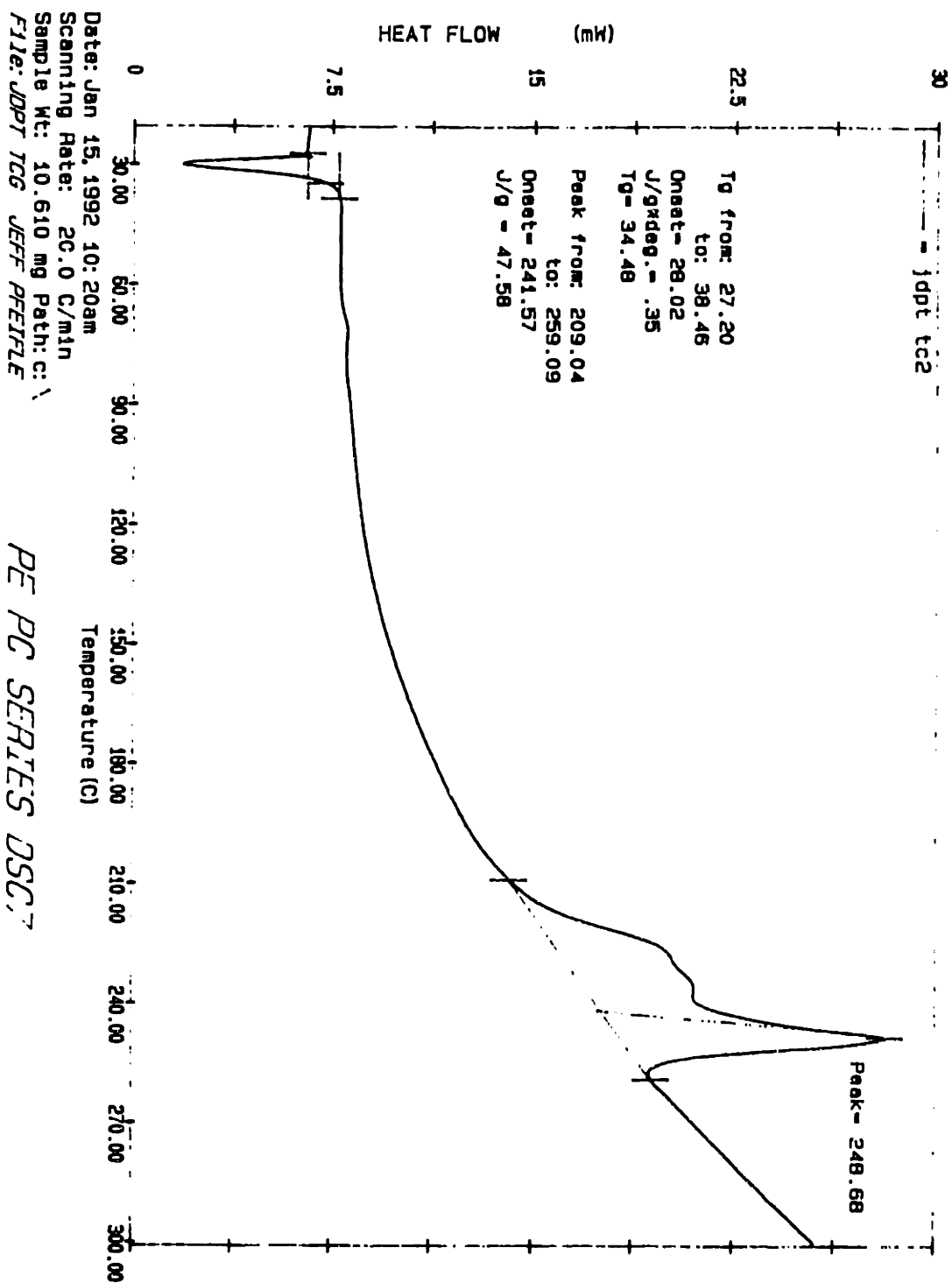
$$m_{as_t} = \left[\frac{4}{3} \cdot \pi \cdot [r_t]^3 \right] \cdot \rho_{\chi} \cdot V_0 \cdot N \cdot \left[1 - \int_0^{2 \cdot r_t} \frac{1}{\sqrt{2 \cdot \pi \cdot \sigma}} \cdot e^{-\left[\frac{r_a - \mu}{2 \cdot \sigma} \right]^2} dr_a \right]$$

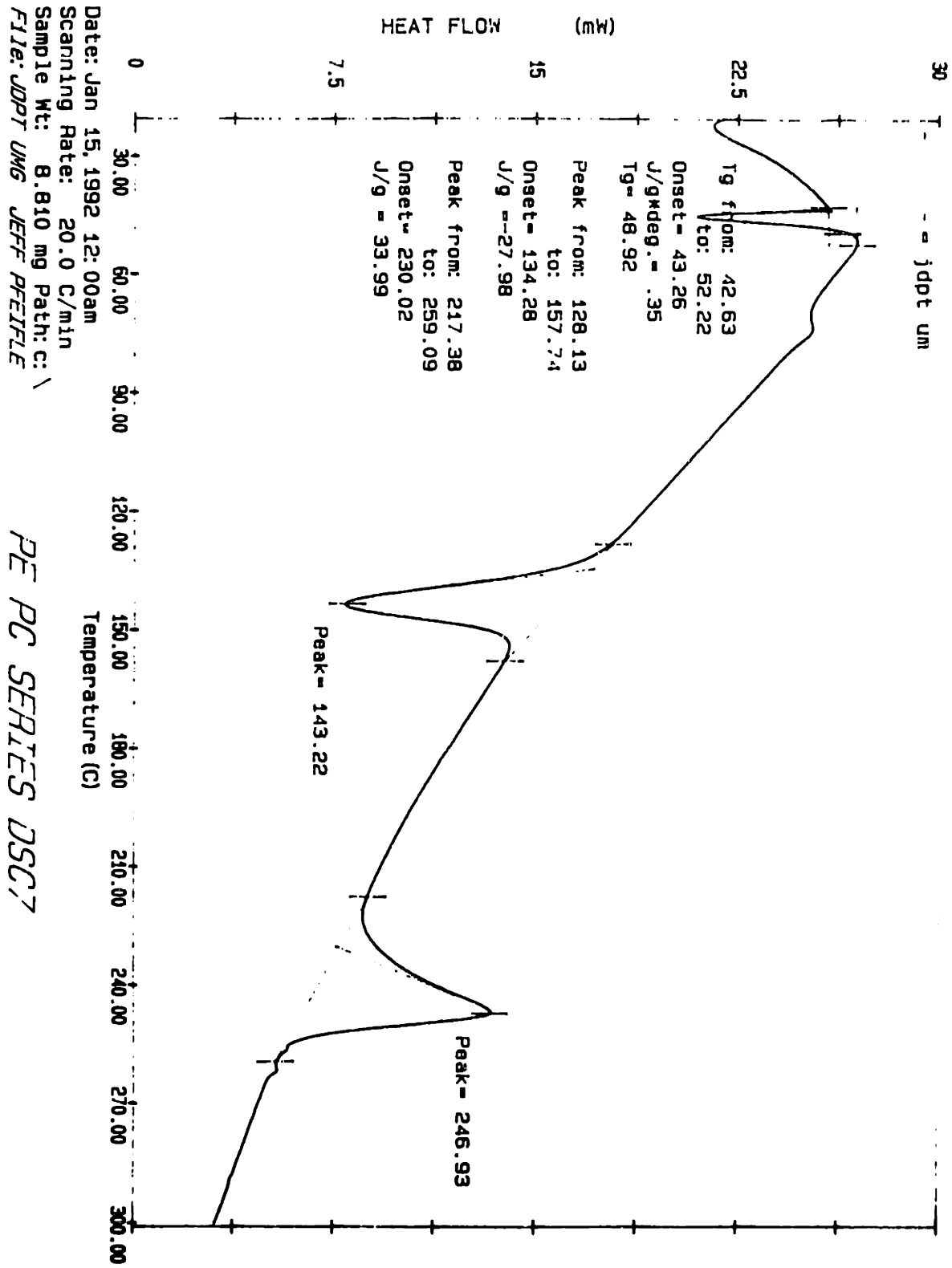
$$m_{is_t} = \int_0^{2 \cdot r_t} \frac{1}{\sqrt{2 \cdot \pi \cdot \sigma}} \cdot \rho_{\chi} \cdot V_0 \cdot N \cdot \left[\frac{4}{3} \cdot \pi \cdot \left[\frac{r_a}{2} \right]^3 \right] \cdot e^{-\left[\frac{r_a - \mu}{2 \cdot \sigma} \right]^2} dr_a$$

$$\chi_t = \frac{m_{as_t} + m_{is_t}}{\rho_{\alpha} \cdot V_0} \quad \text{WRITEPRN(CHIDATA)} = \chi_t$$



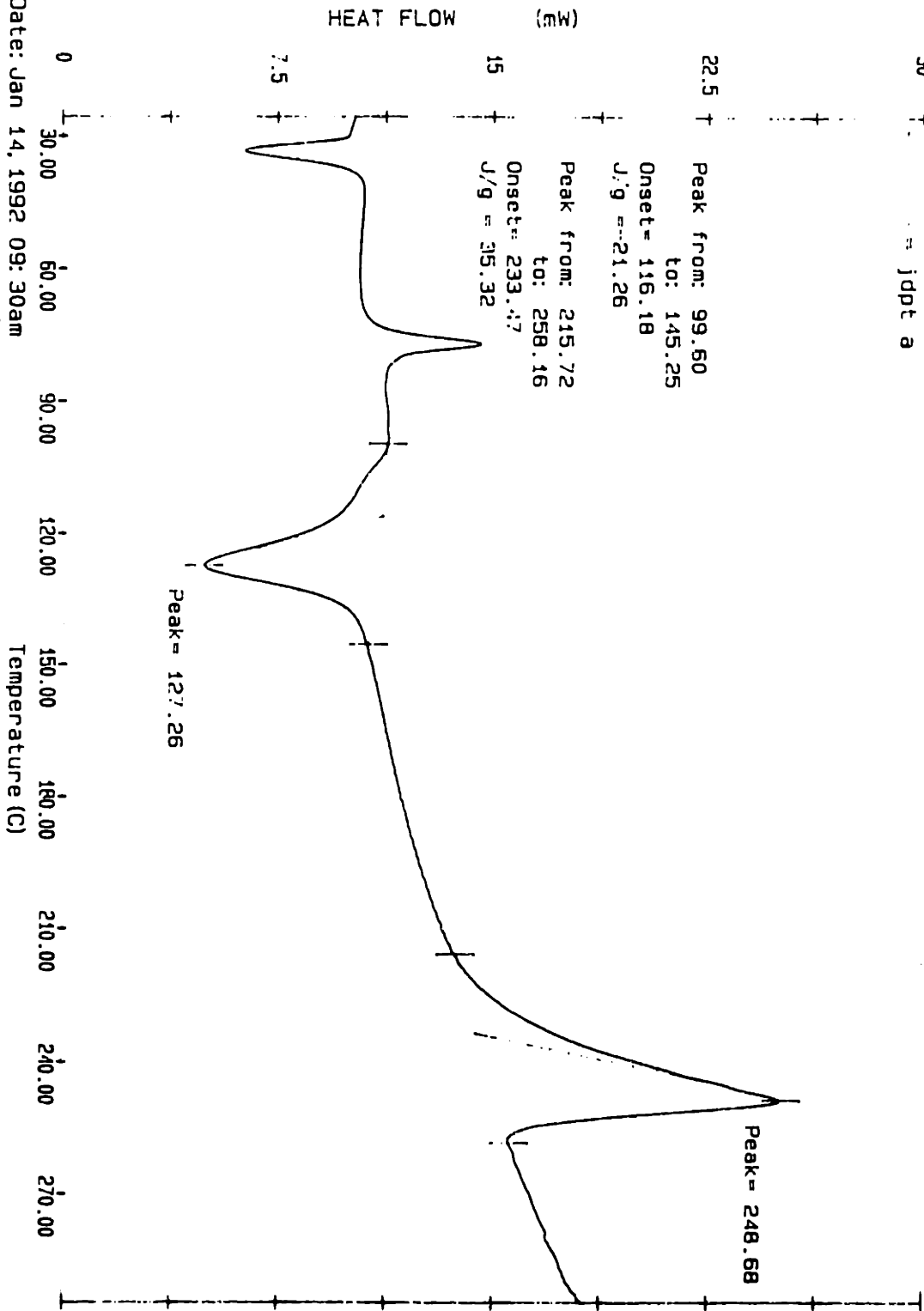
Appendix D - DSC Graphs





PE PC SERIES DSC7

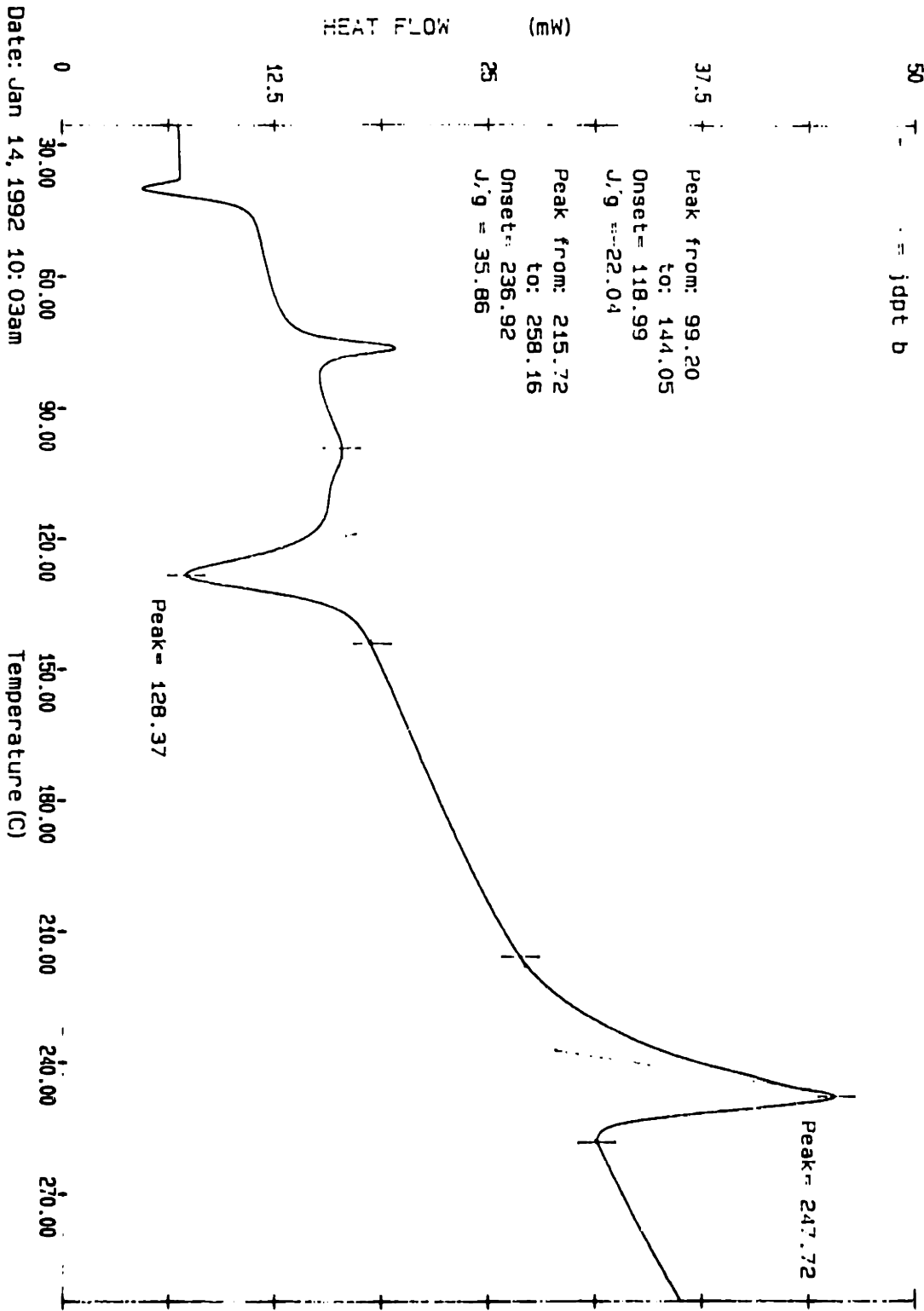
30 T. = jdpt a



Date: Jan 14, 1992 09:30am
Scanning Rate: 20.0 C/min
Sample Wt: 12.090 mg Path: c:\pe\
File: JDPT 4G1 JEFF: PFEI.FIE

PE PC SERIES .DSC?

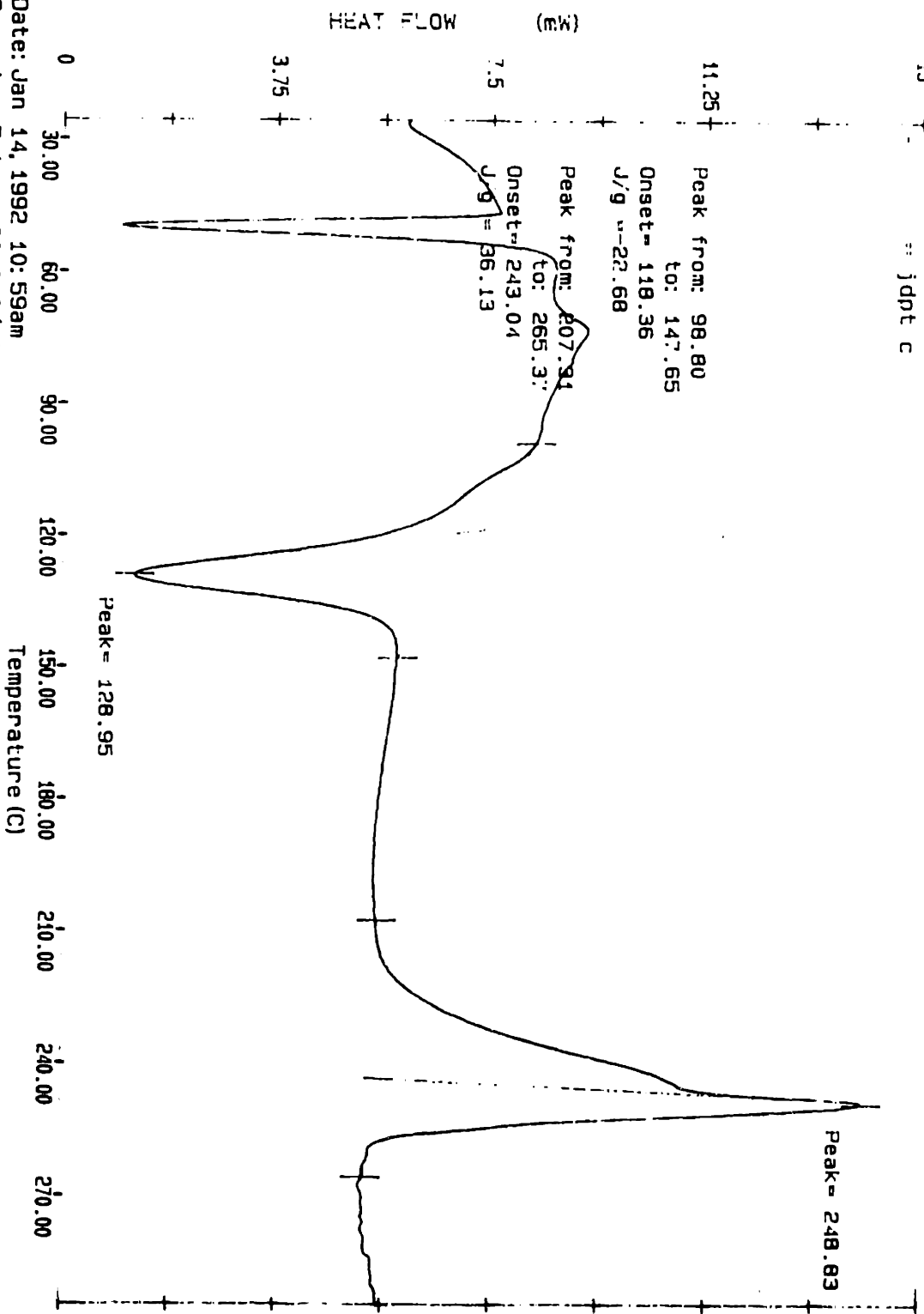
50 T = jdpt b



Date: Jan 14, 1992 10:03am
Scanning Rate: 20.0 C/min
Sample Wt: 17.550 mg Path: c:\pe1
File: JDPT B61 JEFF PEFILE

PE PC SERIES DSC7

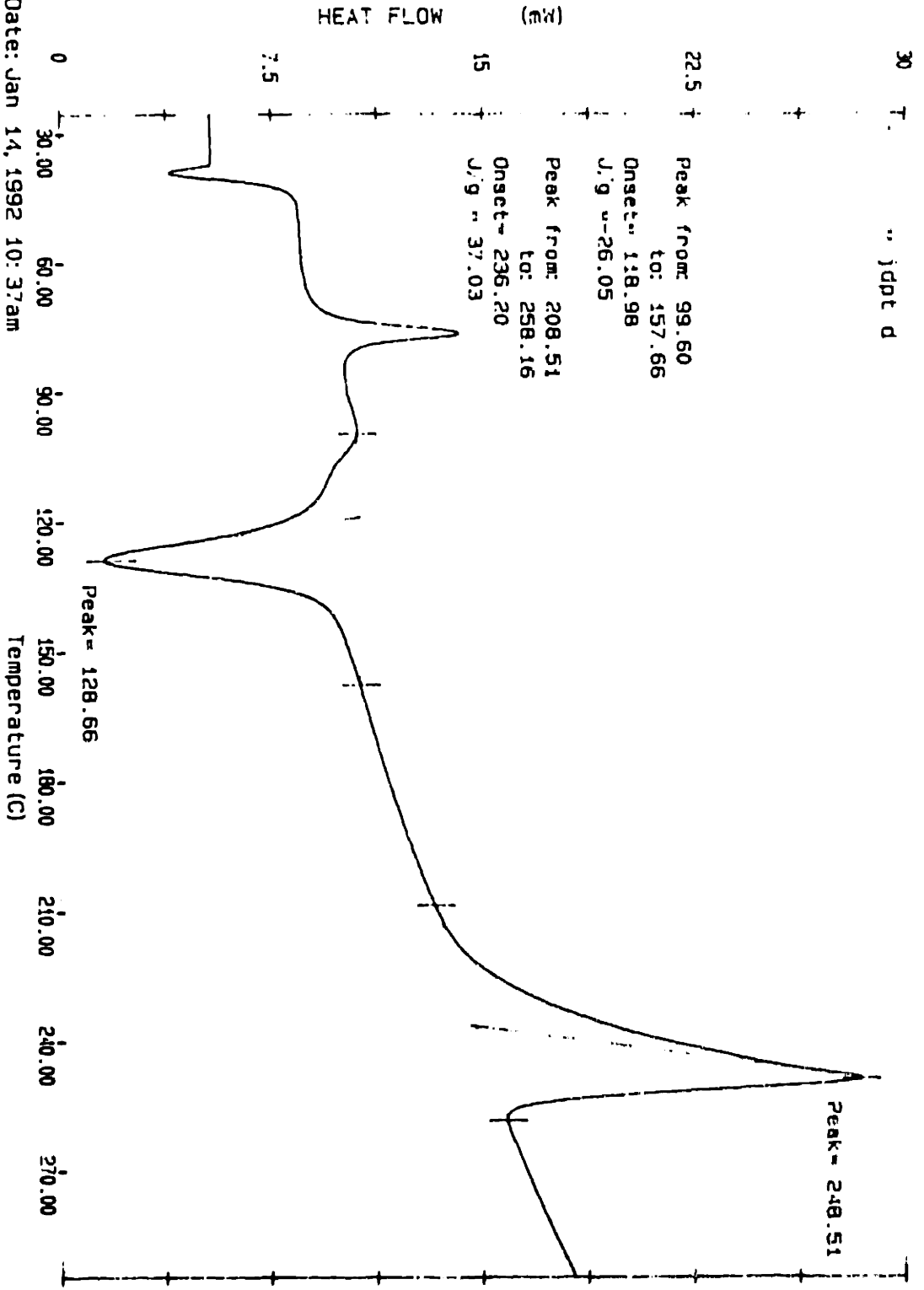
15 T = jdpt c



Date: Jan 14, 1992 10:59am
Scanning Rate: 20.0 C/min
Sample Wt: 10.470 mg Path: c:\pe\
File: JDPT CG1 JEFF PFEIFLE

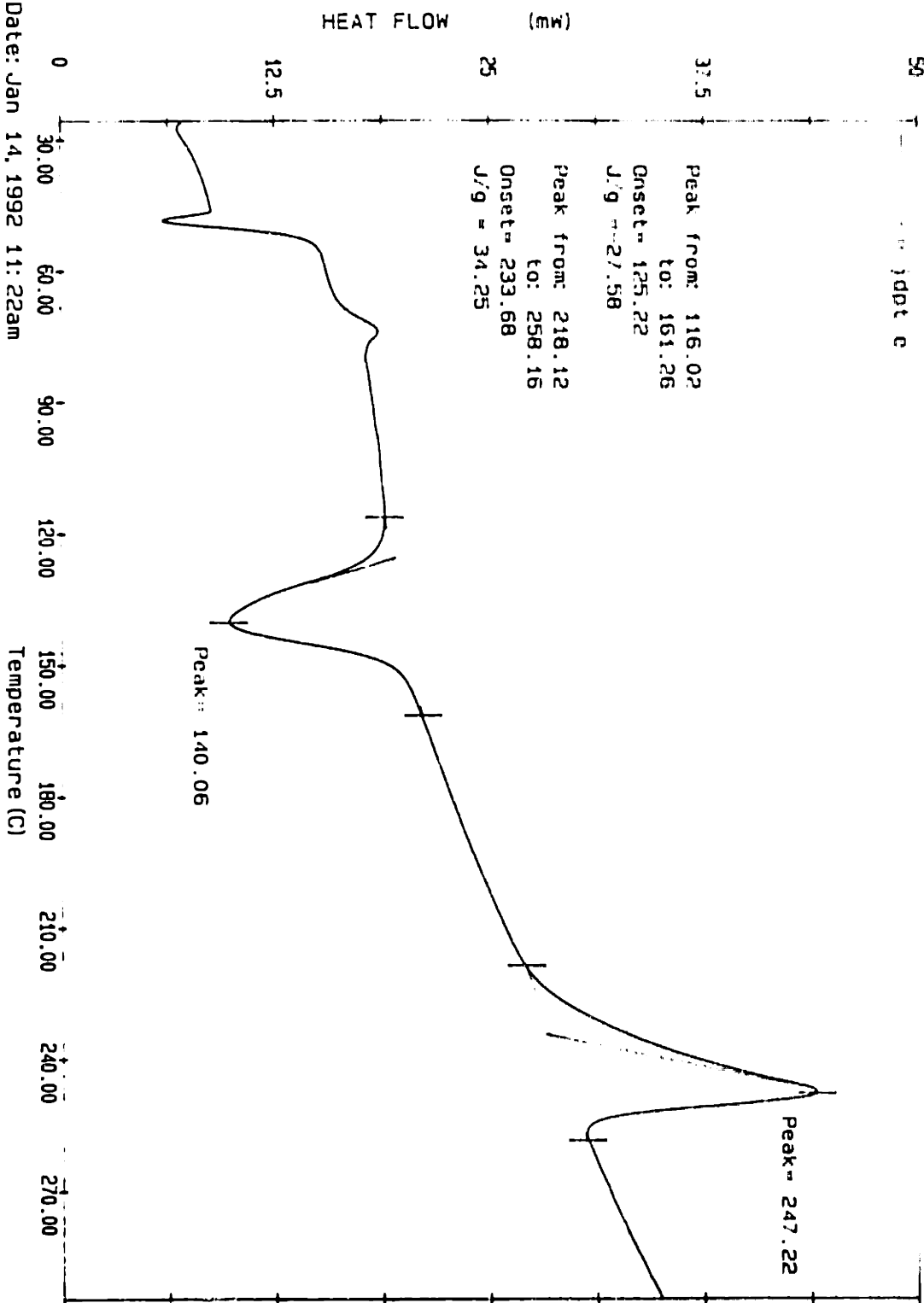
PE PC SERIES DSC7

30 T. " jdppt d



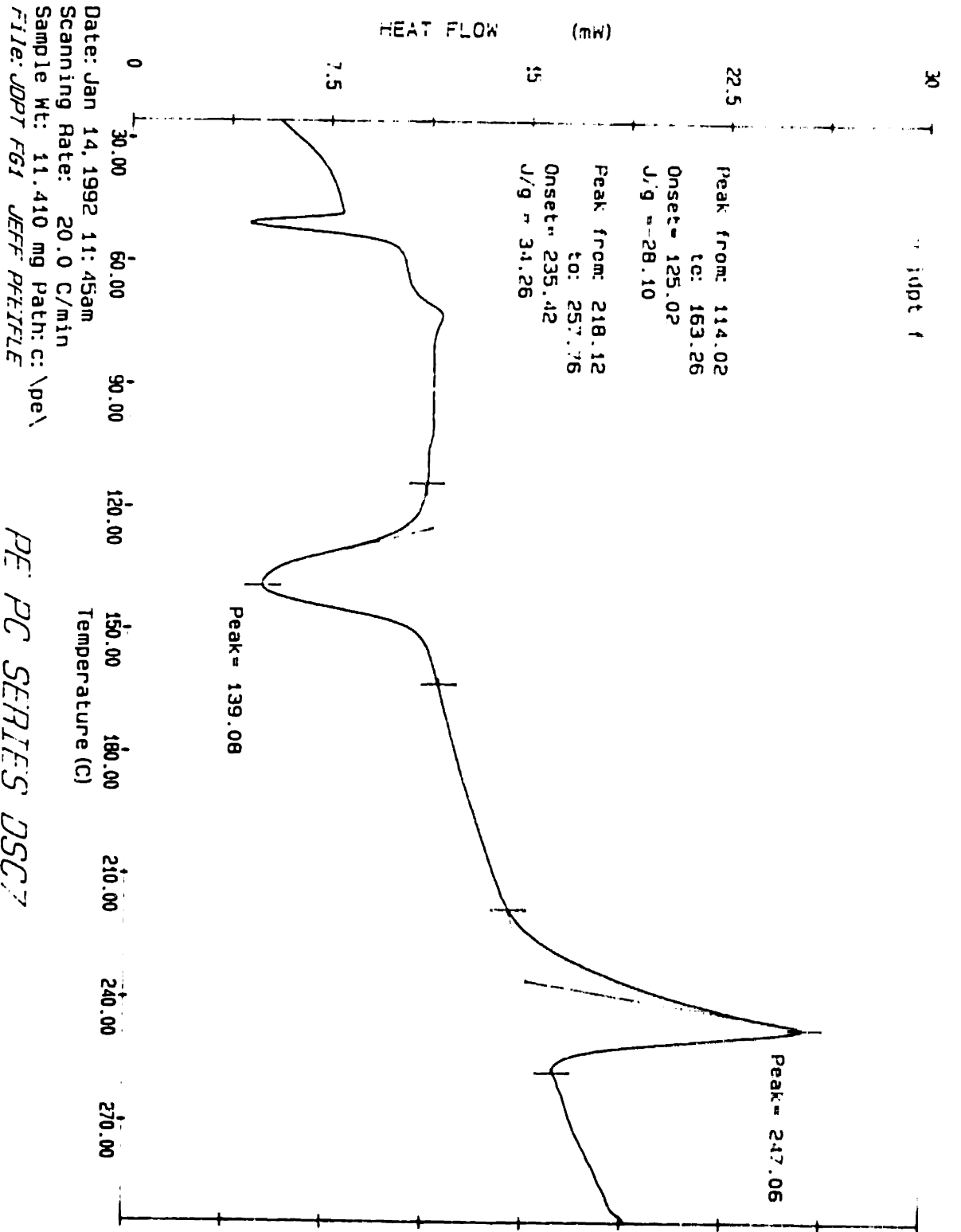
Date: Jan 14, 1992 10:37am
Scanning Rate: 20.0 C/min
Sample Wt: 14.940 mg Path: c:\pe\
File: JDPPT DGI JEFF PFEIFLE

PE PC SEPTIS JSC

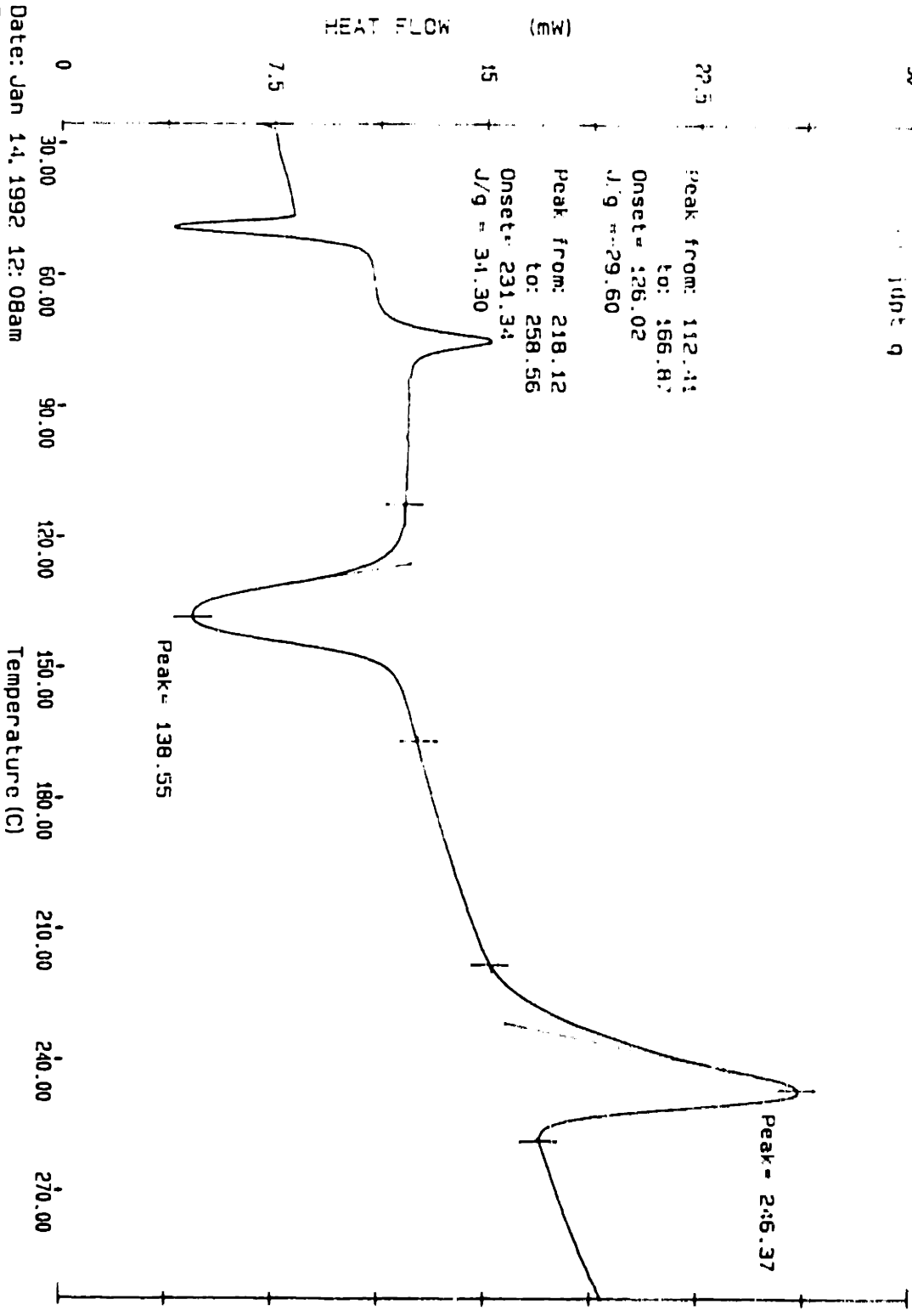


Date: Jan 14, 1992 11:22am
 Scanning Rate: 20.0 C/min
 Sample Wt: 17.510 mg Path: c:\pe\
 File: JDPT EGI JEFF PFEIFLE

PE PC SERIES DSC7

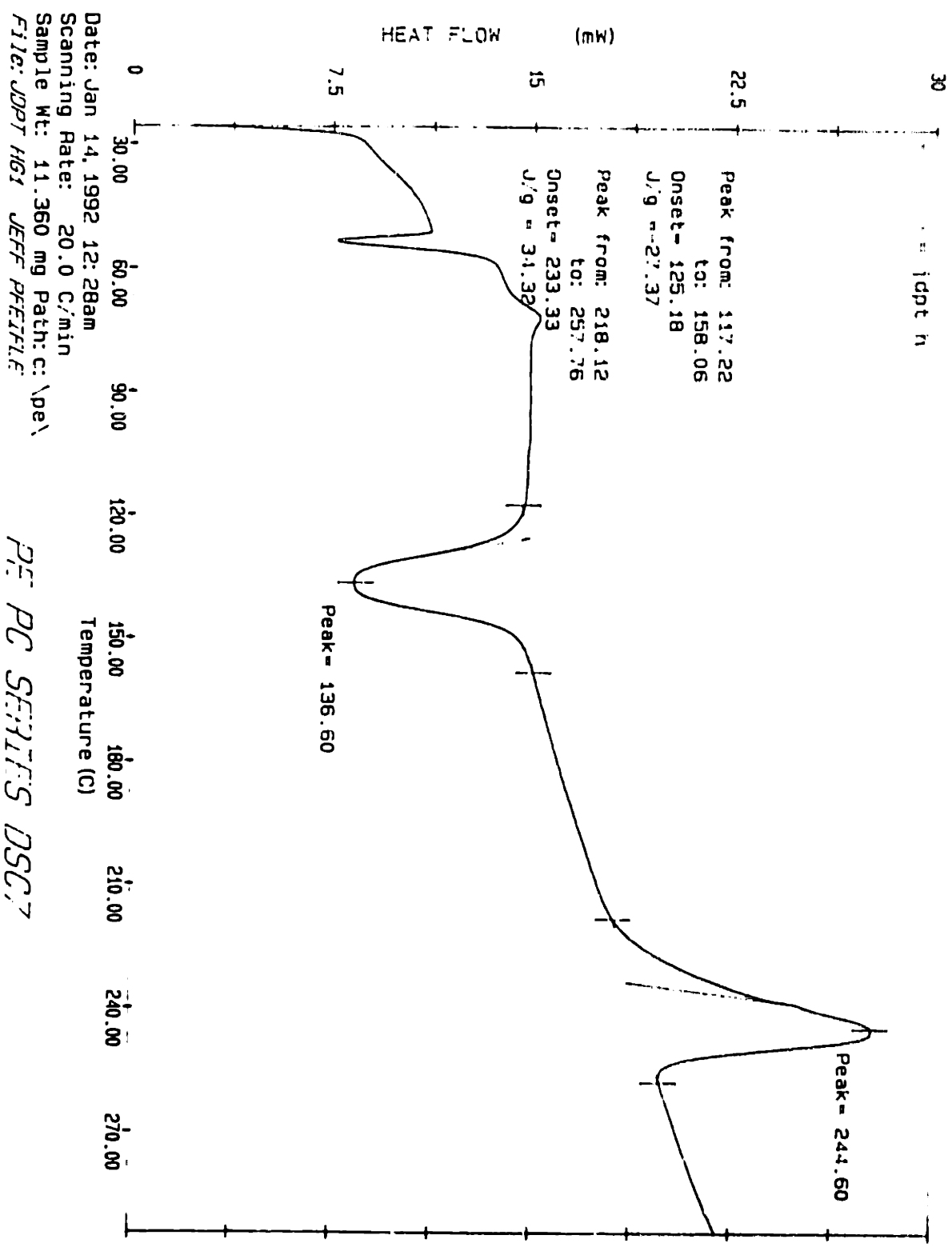


PE PC SERIES DSC7



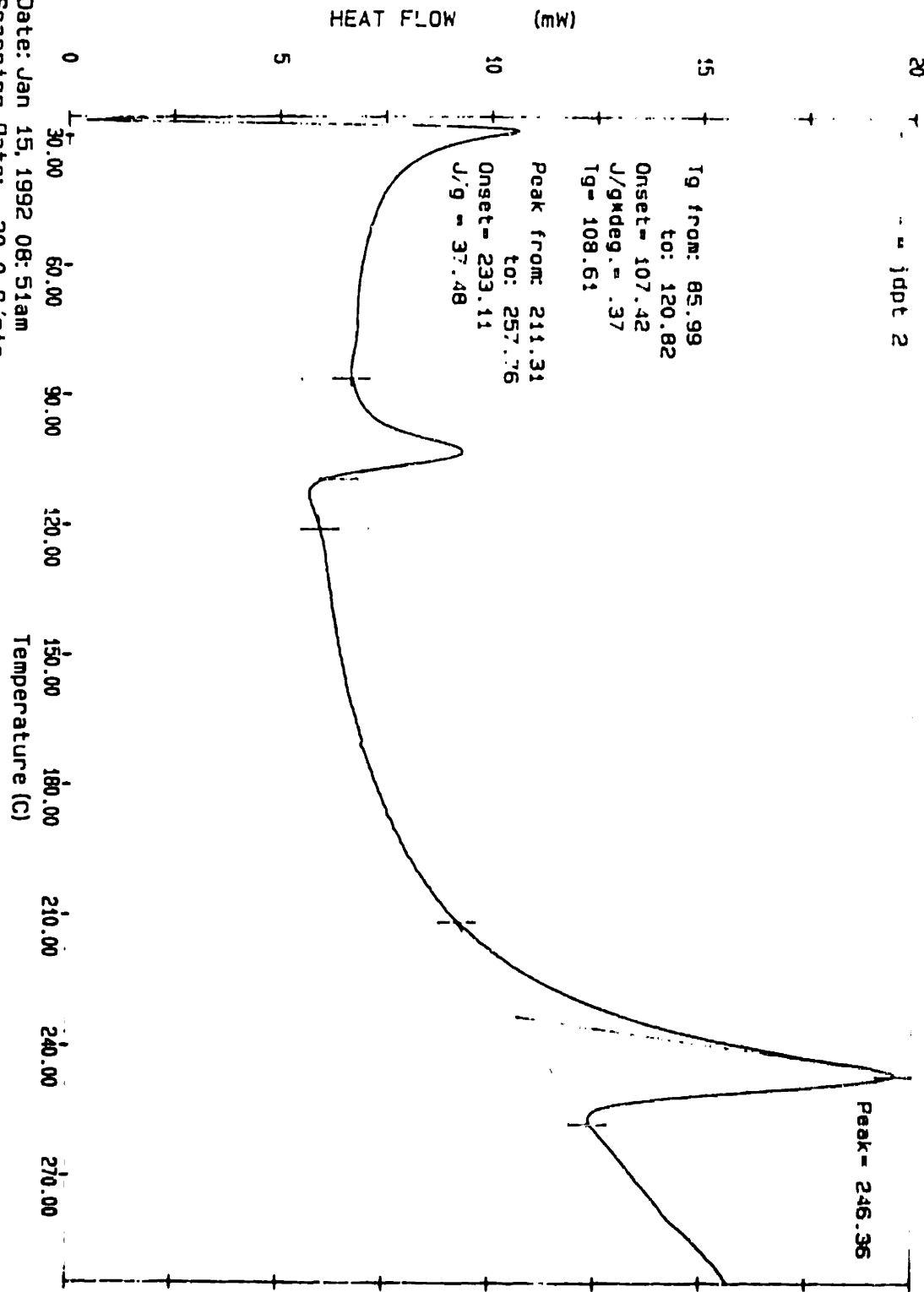
Date: Jan 14, 1992 12:08am
Scanning Rate: 20.0 C/min
Sample Wt: 12.750 mg Path: c:\pe\
File: Jdpt 661 JEFF PEITHLE

PE PC STARTS DSC7



PE PC SEPTIS DSC7

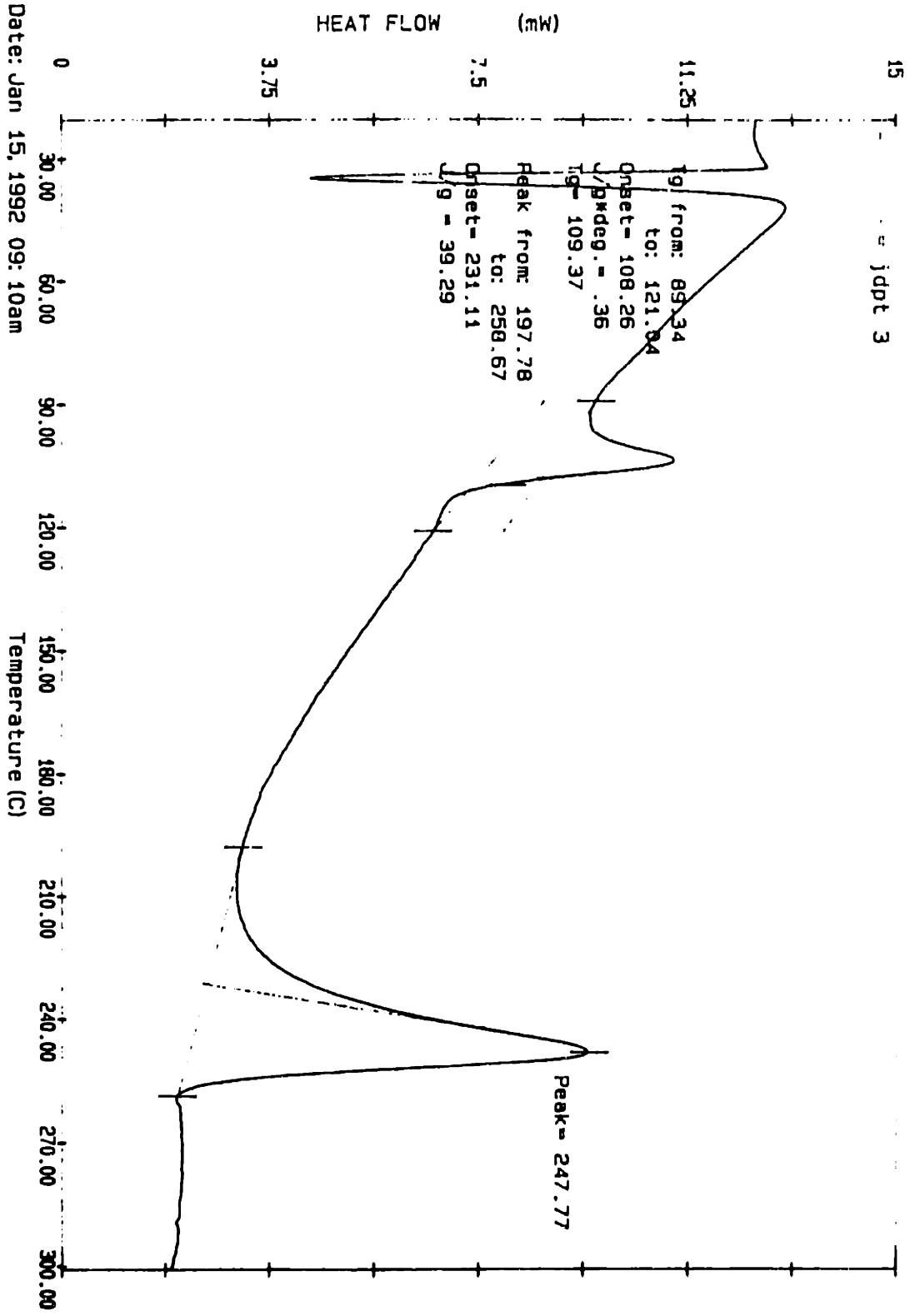
20
- - - jdpt 2



Date: Jan 15, 1992 08:51am
Scanning Rate: 20.0 C/min
Sample Wt: 9.550 mg Path: c:\
File: JDP7 261 JEFF PEETLE

PE PC SERIES DSC7

15
jdpt 3

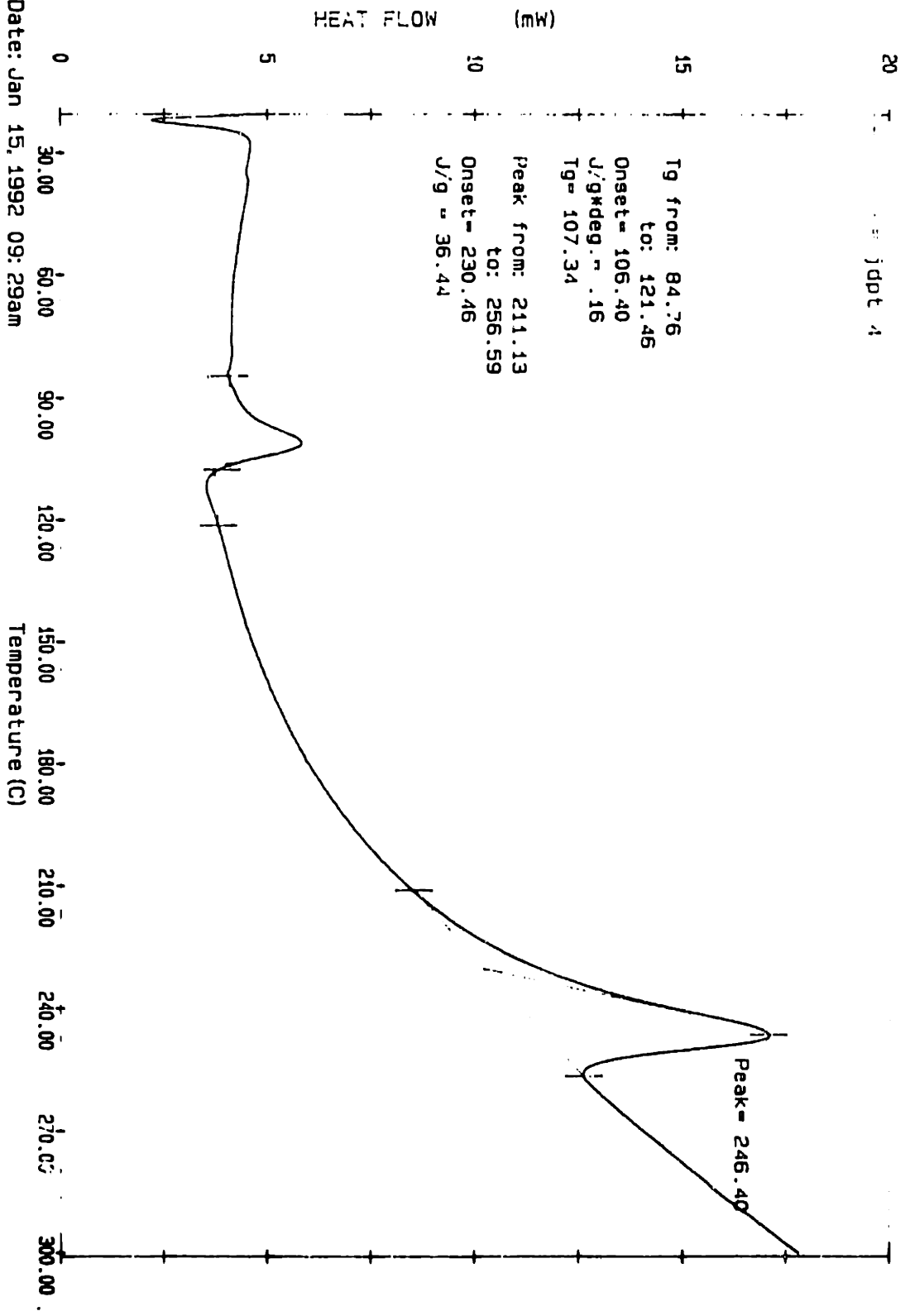


Date: Jan 15, 1992 09:10am
Scanning Rate: 20.0 C/min
Sample Wt: 9.230 mg Path: c:\
File: JDPT 361 JEFF PFEIFLE

PE PC SERIES DSC7

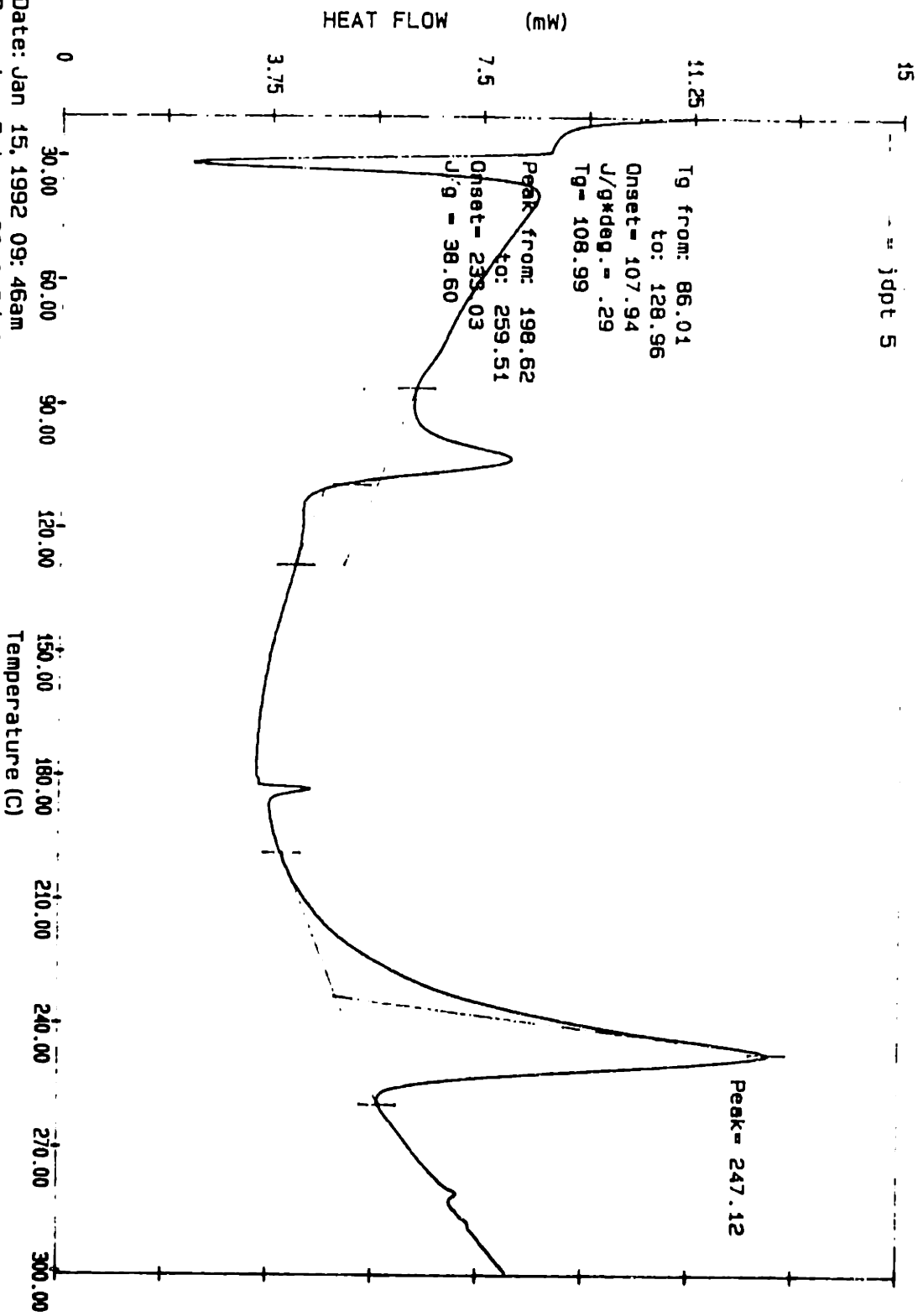
Date: Jan 15, 1992 09:29am
Scanning Rate: 20.0 C/min
Sample Wt: 6.970 mg Path: c:\
File: JDPT 4G1 JEFF PEETFILE

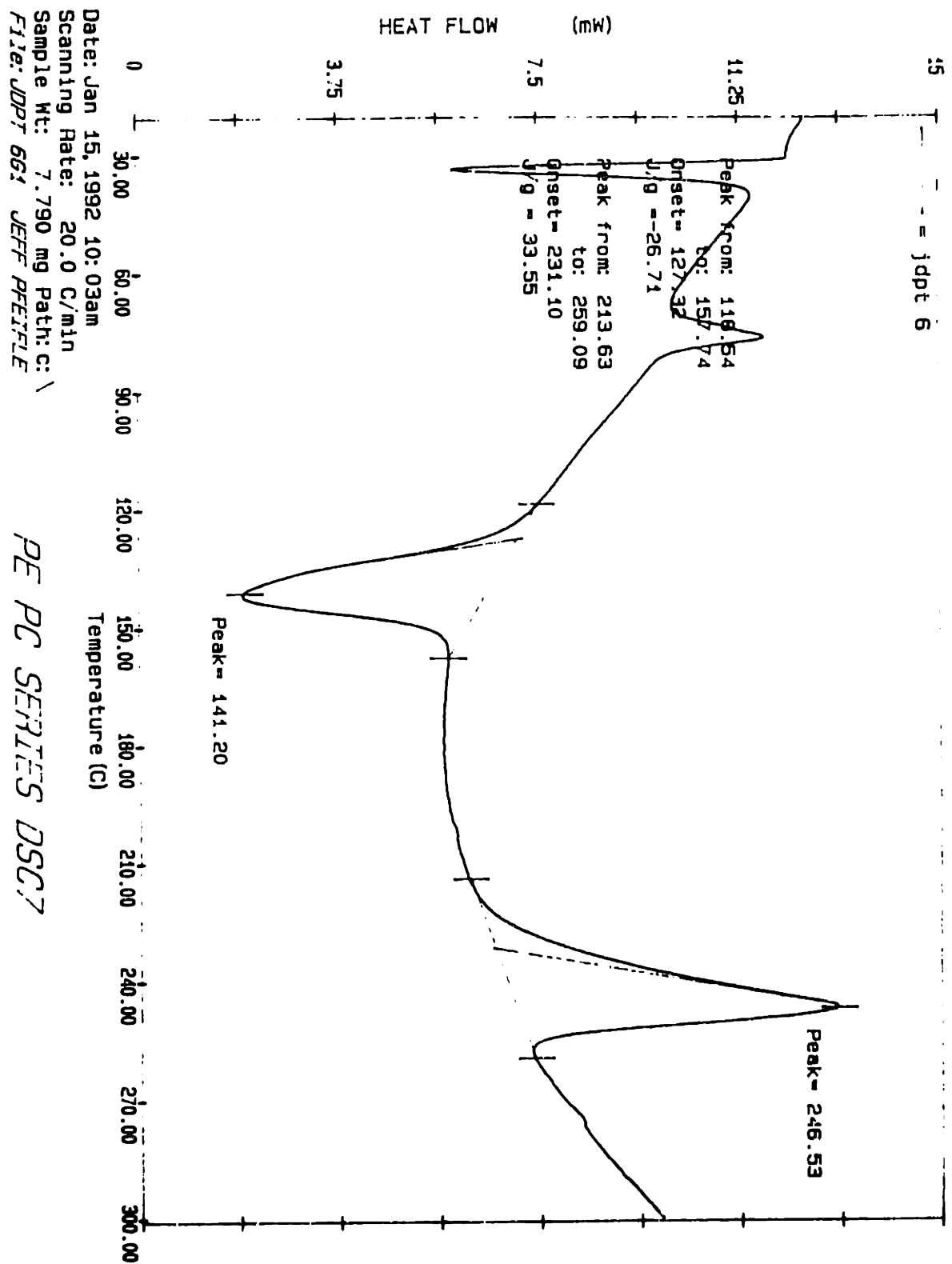
PE PC SERIES DSC7

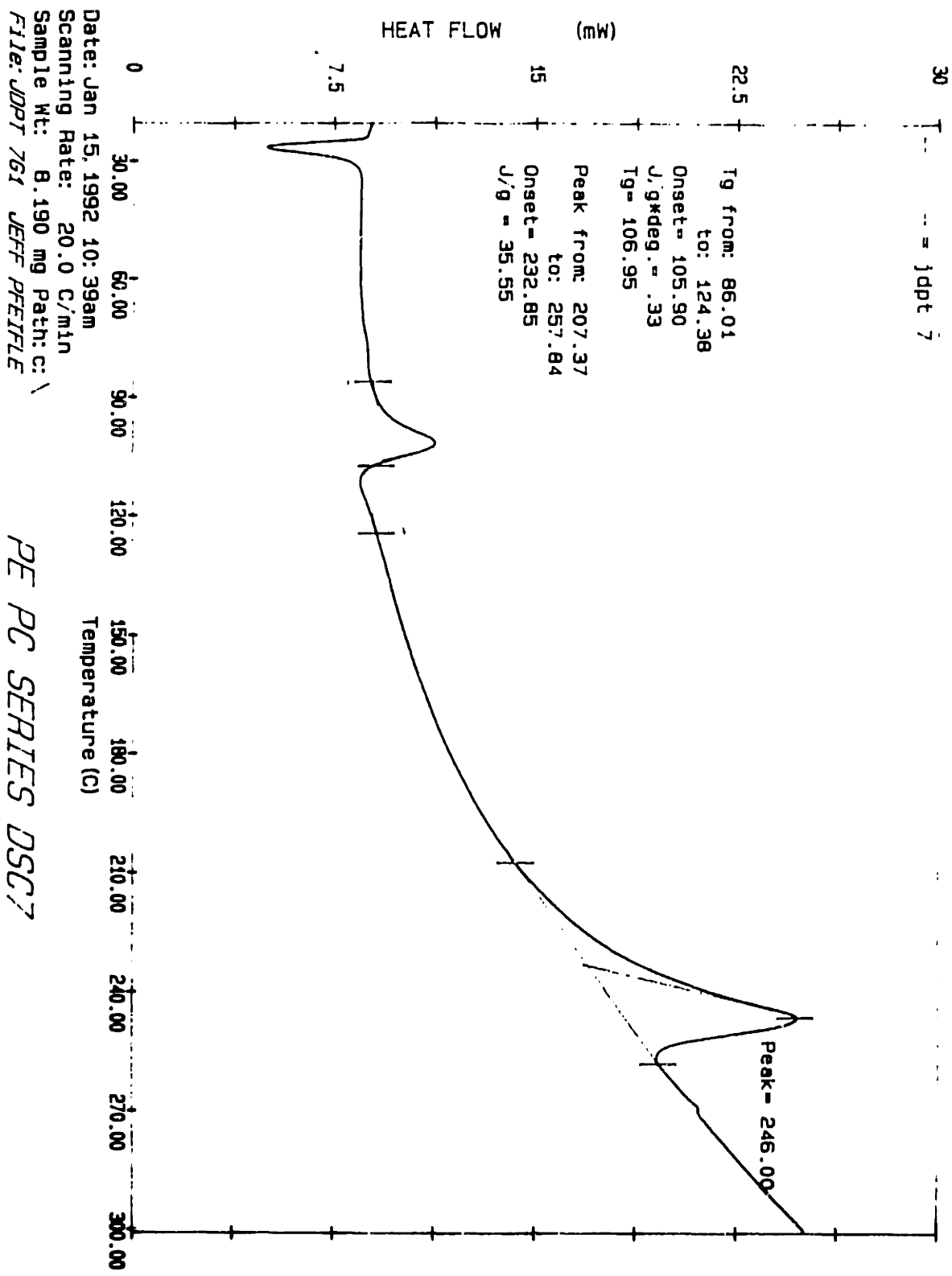


Date: Jan 15, 1992 09: 46am
Scanning Rate: 20.0 C/min
Sample Wt: 8.860 mg Path: c:\
File: JDPT 5G1 JEFF PREIFLE

PE PC SERIES DSC7



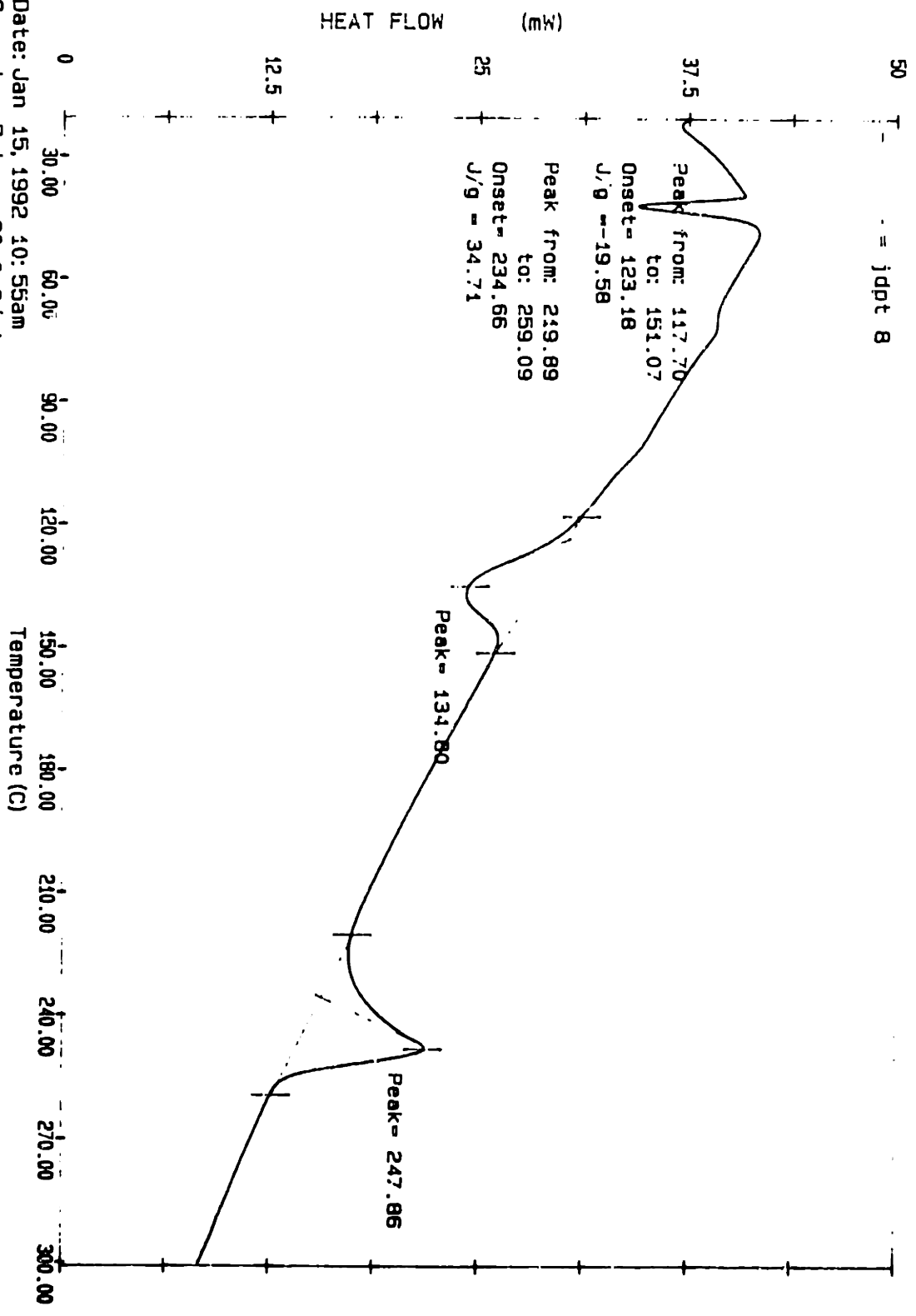


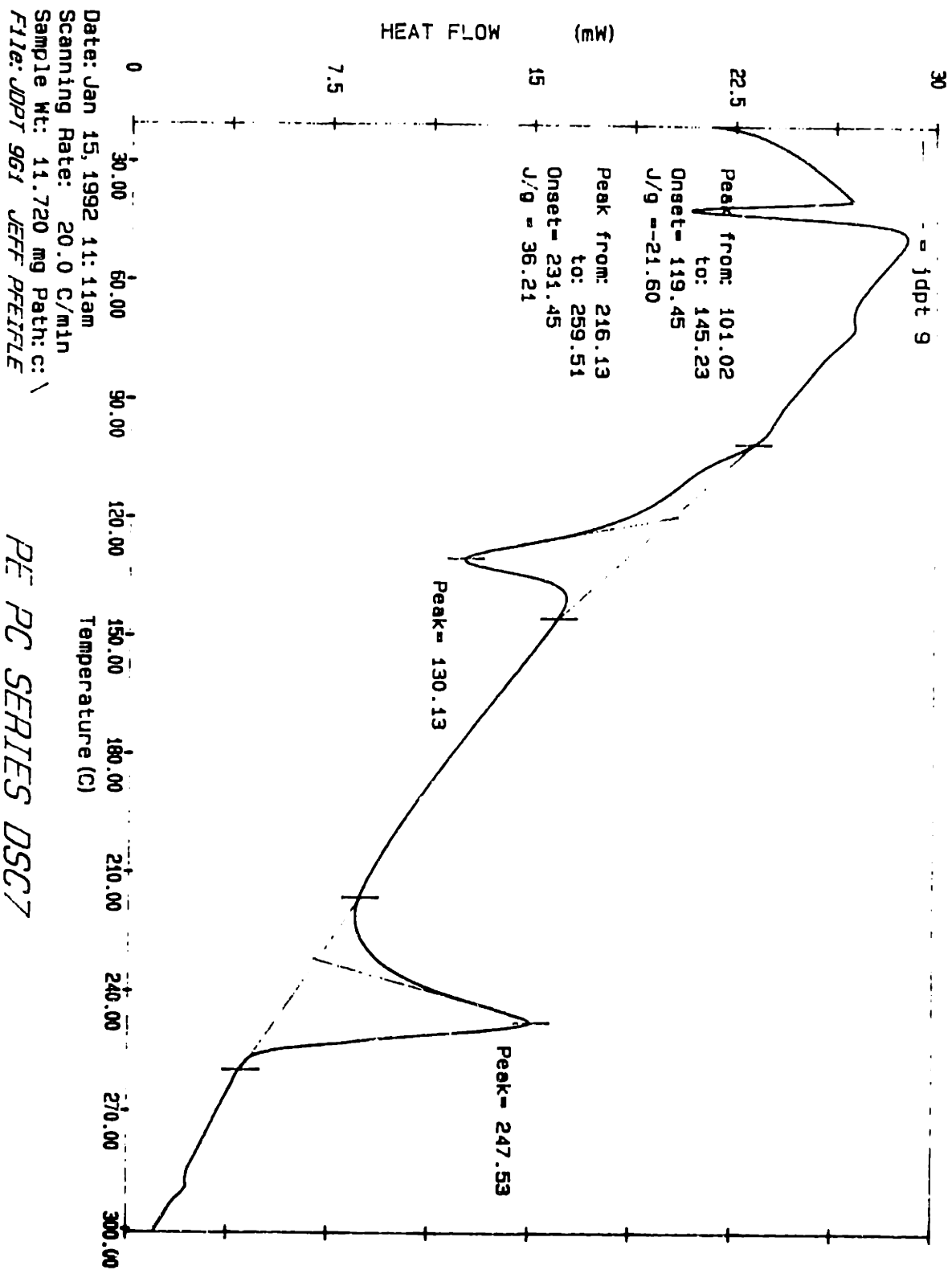


PE PC SERIES DSC7

Date: Jan 15, 1992 10:55am
 Scanning Rate: 20.0 C/min
 Sample Wt: 9.540 mg Path: c:\
 File: JDPT B61 JEFF PEIFILE

PE PC SERIES DSC7

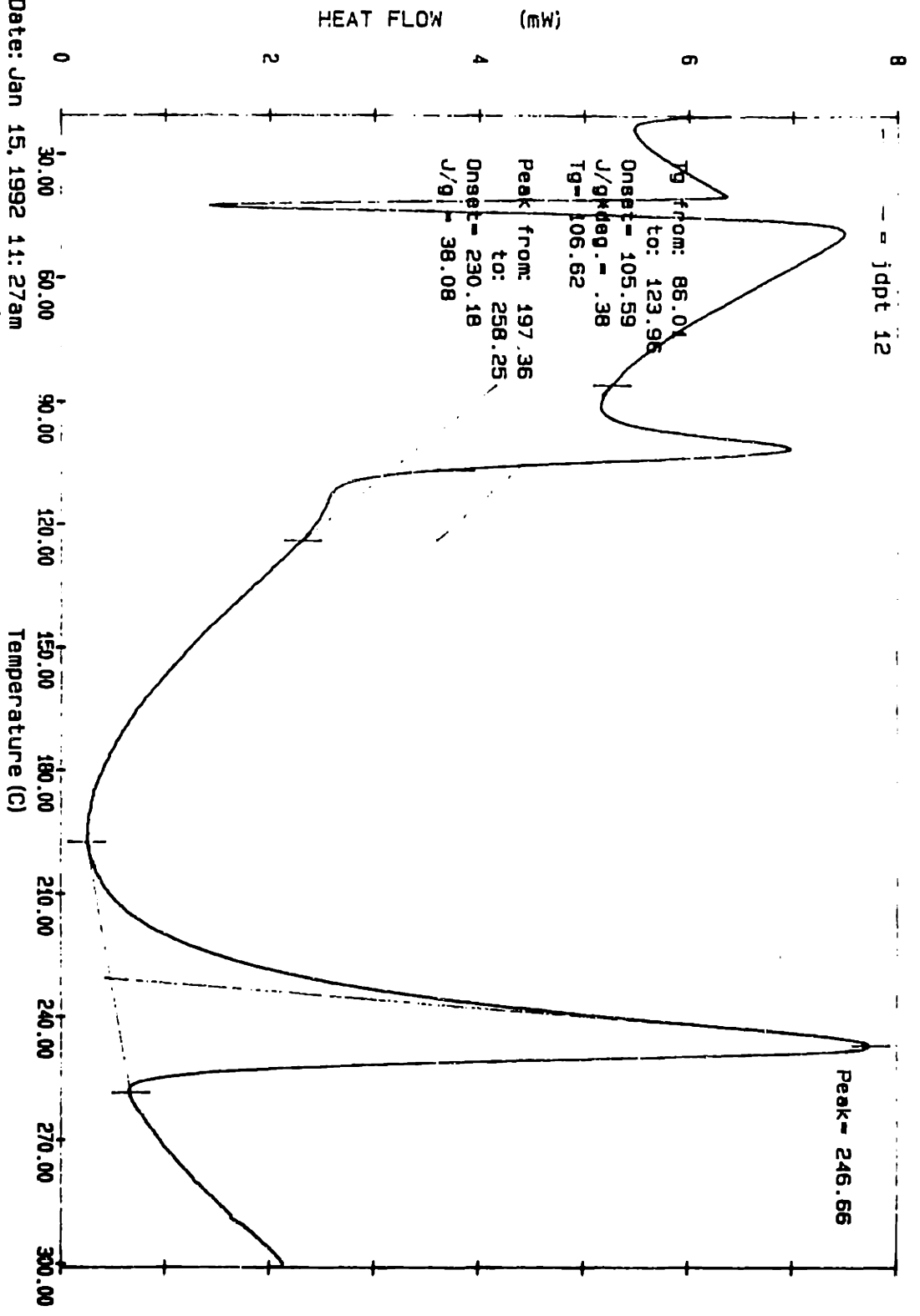




PE PC SERIES DSC7

Date: Jan 15, 1992 11: 27am
 Scanning Rate: 20.0 C/min
 Sample Wt: 9.260 mg Path: c:\
 File: JDP1 126 JEFF PFETILE

PE PC SERIES DSC7



References

- [1] Ashby, M.F. and Jones, D.R.H. *Engineering Materials 1: An Introduction to their Properties and Applications*. Pergamon Press: New York, 1980.
- [2] Ashby, M.F. and Jones, D.R.H. *Engineering Materials 2: An Introduction to their Properties and Applications*. Pergamon Press: New York, 1986.
- [3] Baldwin, D.F. and Suh, N.P. "Modeling Gas Sorption in Semi-Crystalline Polymers." *SPE-ANTEC '91*. SPE: Montreal, Quebec, May 1991.
- [4] Chiou, J.S., Barlow, J.W. and Paul, D.R. "Polymer Crystallization Induced by Sorption of CO₂ Gas." *Journal of Applied Polymer Science*, Vol. 30, 1985.
- [5] Garcia, D. "Heterogeneous Nucleation of Poly(ethylene Terephthalate)." *Journal of Polymer Science: Polymer Physics Edition*, Vol. 22. John Wiley & Sons, Inc.: New York, 1984.
- [6] Heater, P.L. "Polyethylene terephthalate: PET." *Modern Plastics Encyclopedia*. McGraw Hill: New York, 1987.
- [7] Jabarin, S.A. "Crystallization Behavior of Poly(Ethylene Terephthalate)." *Polymer Engineering and Science*, Vol. 29, No. 18, September 1989.
- [8] Kim, S.P. and Kim S.C. "Crystallization Kinetics of Poly(Ethylene Terephthalate). Part I: Kinetic Equation with Variable Growth Rate." *Polymer Engineering and Science*, Vol. 31, No. 2, January 1991.
- [9] Lin, C.C. "The Rate of Crystallization of Poly(Ethylene Terephthalate) by Differential Scanning Calorimetry." *Polymer Engineering and Science*, Vol. 23, No. 3, February 1983.
- [10] Mizoguchi, K., Hirose, T., Maito, Y. and Kamiya, Y. "CO₂ - induced crystallization of poly(ethylene terephthalate)." *Polymer*, Vol. 28, July 1987.
- [11] Muzzy, J.D., Bright, D.G. and Hoyos, G.H. "Solidification of Poly(Ethylene Terephthalate) with Incomplete Crystallization." *Polymer Engineering and Science*, Vol. 18, No. 6, Mid-May 1978.
- [12] Rosen, Stephen L. "Crystallinity." *Fundamental Principles of Polymeric Materials*. John Wiley & Sons, Inc.: New York.
- [13] Schaaf, E and Zimmerman, H. "Non-Isothermal Crystallisation Kinetics of Nucleated Poly(Ethylene Terephthalate)" *Journal of Thermal Analysis*, Vol. 33, 1988.
- [14] Yang, M.C.Y. "Investigation of the Impact Strength of Microcellular Foamed Poly(vinylchloride), Poly(methyl methacrylate), and Polystyrene Sheet." S.B. Thesis in Mechanical Engineering. MIT, June 1991.
- [15] Yannas, I.V. and Luise, R.R. "The Strophon Theory of Deformation of Glassy Amorphous Polymers: Application to Small Deformations." *The Strength and Stiffness of Polymers*. Marcel Dekker: New York, 1983